Investigating the Biological Role of O-Acyl ADP Ribose

by Elyse Blazosky

A thesis submitted to Johns Hopkins University in conformity with the requirements for the degree of Master of Science

Baltimore, Maryland
November, 2018

© Elyse Blazosky
All Rights Reserved

Abstract

Sirtuins are an ancient family of deacetylase enzymes found in all three domains of life, where they have diverse biological roles. These widely studied enzymes are popular drug targets for treating diseases associated with aging, neurological disorders, cardiovascular disorders, metabolic disorders and even cancer. Unlike most deacetylase enzymes which use water to hydrolyze the amide bond linking the acetyl group to a lysine side chain, sirtuins catalyze a unique NAD^+-dependent reaction that yields O-acetyl ADP ribose, nicotinamide and the deacetylate lysine. This seemingly wasteful use of NAD^+ has led some to hypothesize that sirtuin activity is coupled to NAD^+ levels in the cell. While sirtuin activity does rely on NAD^+ biosynthesis and salvage pathways, it is unclear whether NAD^+ levels fluctuate to a level that could affect sirtuin activity in-vivo. More recent studies have revealed new roles for sirtuins which suggests a more complex role of the sirtuin and a re-evaluation of the current hypothesis for why sirtuins uses NAD^+. It has been shown that some sirtuins preferentially remove a variety of acyl lysine groups such as malonyl, succinyl, and butyryl, forming the corresponding O-acyl ADP ribose product. Mass spectrometry studies have revealed an abundance of these acyl modifications on cellular proteins, some of which are thought to result from non-enzymatic reaction with metabolites such as acyl-CoAs. I hypothesize that sirtuins use NAD^+ to generate a carrier molecule (ADP ribose) to shuttle the leaving acyl chain to downstream metabolic pathways. This thesis focuses on progress made testing this hypothesis including the synthesis, purification and stability of ^{13}C-labeled O-succinyl ADP ribose, as well as preliminary mass spectrometry metabolomics studies.

Thesis Advisor:

Dr. Cynthia Wolberger, Ph.D
Professor
Department of Biophysics and Biophysical Chemistry

Thesis Reader:

Dr. Namandje Bumpus, Ph.D
Associate Professor; Associate Dean for Basic Science Research
Division of Clinical Pharmacology

Acknowledgments

To Dr. Cynthia Wolberger, for your time and the many lessons I learned from you.

To the members of the Wolberger Lab, for your support of both me and this project.

To Dr. Namandje Bumpus, for inviting me into your lab, and for your mentorship.

To the members of the Bumpus Lab, in particular Ms. Carley Heck, for treating me as a member of the lab, and for your guidance with mass spectrometry.

To Dr. Ananya Majumdar, for your unconditional friendship.

To Mr. Anthony Veltri, for tea walks.

To Mr. Brendan Long, for not eating my bear claws too many times while I was writing this thesis, and for your love.

To Dr. Don Wilmes, for helping me remember who I really am.

To Mrs. Elizabeth Harrison, for your wisdom.

Table of Contents

List of Figures

List of Abbreviations

Adenosine monophosphate (AMP)

Adenine dinucleotide (ADP)

Adenine dinucleotide ribose (ADPr)

Coenzyme A (CoA)

Histone deacetylase (HDAC)

Matrix Assisted Laser Desorption/Ionization Time-of-Flight Mass Spectrometry (MALDI-TOF)

Mass to charge ratio (*m/z*)

Michalis constant (K_M)

Nicotinamide adenine dinucleotide (NAD^+)

O-acyl ADP ribose (O-acyl ADPr)

O-succinyl ADP Ribose (O-succinyl ADPr)

Retention Time (RT)

Liquid chromatography mass spectrometry (LC-MS)

Liquid chromatography tandem mass spectrometry (LC-MS/MS)

Chapter 1

Introduction and Background

1.1 Sirtuins

Sirtuins are a universally conserved family of nicotinamide adenine dinucleotide (NAD^+) - dependent deacetylase enzymes. These enzymes are widely studied because of their diverse roles in biology and disease (Guarente 2018). Sirtuins are key players in a vast array of biological processes such as lipogenesis, glucose metabolism, circadian clock regulation, transcriptional regulation, cell autophagy, and DNA damage response (Sebastian, Satterstrom et al. 2012). For example, the mammalian sirtuin, SIRT1, deacetylates forkhead box O proteins (FOXO), which activates genes involved in stress response (Xiong, Salazar et al. 2011), while the mammalian sirtuin, SIRT2, can deacetylate alpha-tubulin thereby signaling the recruitment of transport complexes such as kinesin and dynein (Reed, Cai et al. 2006). Because of their diverse roles, sirtuins are attractive drug targets (Kane and Sinclair 2018) and are implicated in many diseases including age-related diseases such as neurodegeneration (Szegő, Outeiro et al. 2018), mood and metabolic disorders (Alageel, Tomasi et al. 2018), and cardiovascular disease (Ma and Li 2015), as well as pathological contexts including the inflammatory response (Vachharajani, Liu et al. 2016), bacterial infection (Eskandarian, Impens et al. 2013) and HIV-1 transcription (Pinzone, Cacopardo et al. 2013).

Sirtuins comprise an ancient class of enzymes found in all three domains of life. All sirtuins contain a 250 amino acid conserved catalytic core domain with varying N and C terminal extensions (Frye 2000). Most archaea and bacteria have one or two sirtuins while mammals have more. Humans have seven sirtuins (SIRT1-7), and budding yeast have five including the

founding member, Sir2 (Shore, Squire et al. 1984). These yeast sirtuins are functionally non-redundant, and found in different subcellular compartments within the cell.

1.2 Sirtuin Structure

The 250 amino acid catalytic core domain is divided into two main subdomains. The large subdomain adopts a canonical Rossmann fold, which is a mononucleotide binding motif found in many enzymes that bind NAD^+/NADH or $NADP^+$/NADPH (Rossmann and Argos 1978). The smaller domain, a zinc binding module, contains four conserved cysteines that coordinate a structured zinc atom. Both the acetylated lysine substrate and NAD^+ bind in a cleft between the two domains. The peptide around the acetylated lysine forms β -sheet contacts with residues from both the large and small subunit. These contacts bring the subunits closer together and is sometimes referred to as the β-staple (Avalos, Celic et al. 2002). The β - staple positions the acetyl lysine in a conserved hydrophobic tunnel, where the lysine side chain forms van der Waals interactions with conserved aliphatic residues. This also places acetyl chain near the catalytic histidine and the NAD^+ binding site.

NAD^+ also binds in the cleft between the two subdomains (Hoff, Avalos et al. 2006). Kinetic studies have revealed (Borra, Langer et al. 2004) that the acetylated lysine binds first, facilitating a closed conformation of the sirtuin (Cosgrove, Bever et al. 2006) allowing NAD^+ to bind. Additionally, (Avalos, Celic et al. 2002) discovered the nicotinamide ring on NAD^+ samples a variety of conformational states, and does not settle into the correct position in the highly conserved, 'C-pocket', until the acetyl-lysine has bound. The 'C-pocket' contacts the nicotinamide ring with van der Waals interactions and places a steric constraint on the ring

allowing for a more energetically favorable removal during catalysis (Sauve, Wolberger et al. 2006).

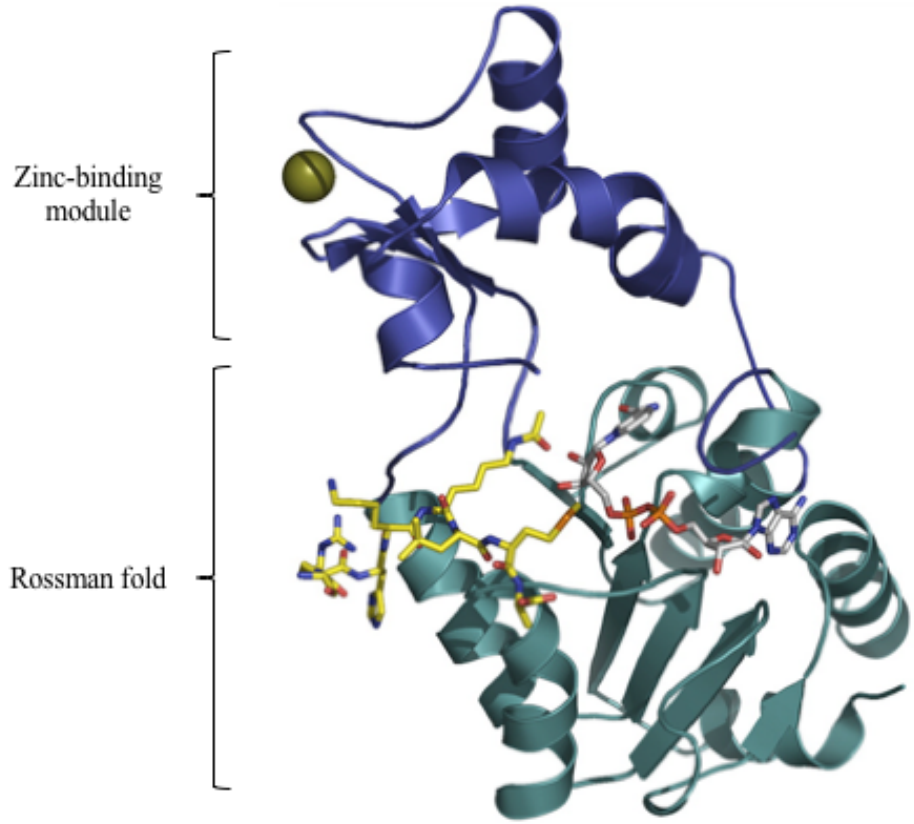

Figure 1.1 Bacterial sirtuin, Sir2Tm, bound to NAD^+ and acetylated peptide. NAD^+ (grey) and acetylated peptide (yellow) sit in the cleft between the zinc-binding module (blue) and Rossman fold (teal). Figure from (Hoff, Avalos et al. 2006).

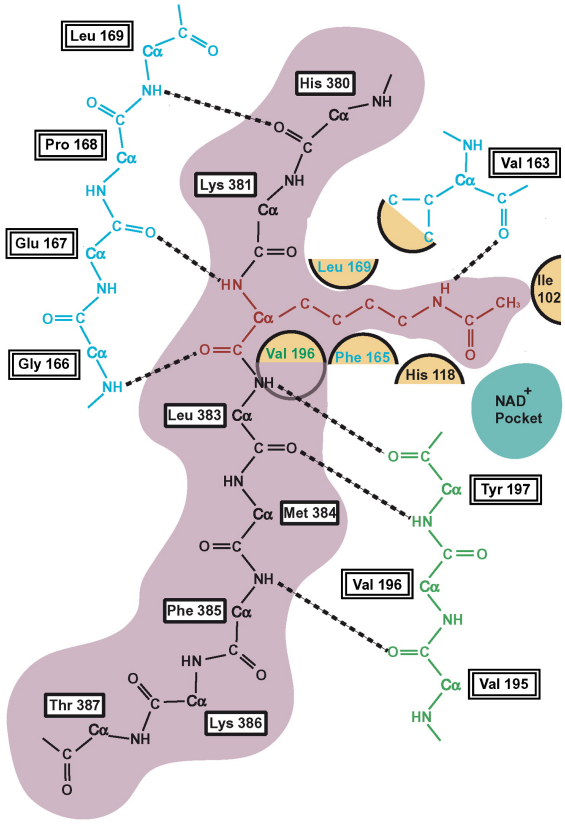

Figure 1.2 Sirtuin binding interaction with acetylated lysine peptide. Peptide backbone (black) hydrogen bonding interactions with sirtuin, Sir2-Af2 (green and blue). Acetylated lysine (red) burrows in the hydrophobic tunnel (yellow) of the sirtuin. Figure from (Avalos, Celic et al. 2002)

1.3 Sirtuin Reaction Mechanism

Once both substrate and NAD^+ are bound, the sirtuin can catalyze the unique NAD^+ -dependent de-acetylation reaction. A detailed explanation the reaction mechanism can be found in (Sauve, Wolberger et al. 2006) and (Bheda, Jing et al. 2016). During the first step, the acetyl lysine serves as a nucleophile, which attacks the 1' position of NAD^+. The nicotinamide group is released, forming an ADP-ribosylated alkylamidate intermediate between the ADP ribose (ADPr) and the acetyl-lysine (fig 1.3 step I). Following this, a conserved histidine residue acts a general base to deprotonate 2'-oxygen, which can attack the acetyl carbonyl carbon forming the cyclic O-alkyamidate intermediate (fig 1.3 step II). The cyclic intermediate resolves by most likely an SN_1-like or dissociative reactive mechanism where an activated water molecule attacks the cyclic O-alkylamidate intermediate, a proton is extracted by the ε-nitrogen of the lysine substrate, and the unmodified lysine is released (fig 1.3 steps III). The resulting products are unmodified lysine and the 2' O-acetyl ADP ribose (O-acetyl ADPr), which can isomerize to 3' O-acetyl ADPr.

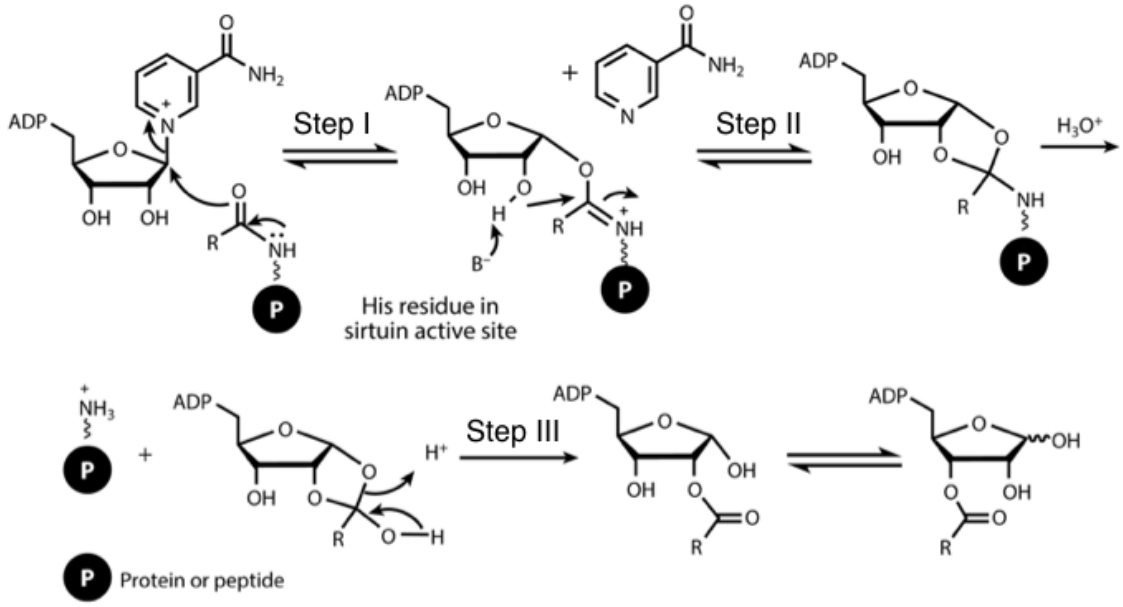

Figure 1.3 Sirtuin catalyzed deacetylation reaction mechanism. Step I: Cleavage of nicotinamide from NAD^+. Step II: Formation of the O-alkylamidate cyclic intermediate. Step III: Resolution of the intermediate by hydrolysis via an activated water molecule to form 2' O-acetyl ADPr, which can isomerize to 3' O-acetyl ADPr. Figure from (Bheda, Jing et al. 2016).

1.4 NAD^+-Dependent Deacetylation

The most striking feature of sirtuin chemistry is the NAD-dependent deacetylation reaction mechanism which converts NAD^+ to the unusual molecule, O-acetyl ADPr. Sirtuins are the only member of the histone deacetylase (HDAC) super family to use the cosubstrate NAD^+; other HDAC enzymes simply use water to hydrolyze the acetyl-lysine isopeptide bond. The energy released by hydrolysis of NAD^+ is 8.2 kcal/mol. This is comparable to the hydrolysis of ATP to ADP at roughly 7.3 kcal/mol (Tong and Denu, 2010). The mystery of why sirtuins, an evolutionarily conserved enzyme found in all three domains of life uses the energetically expensive molecule, NAD^+, is an ongoing discussion in the literature.

A common hypothesis justifying the use of this cofactor is that, by consuming NAD^+, sirtuins act as metabolic sensors that couple protein deacetylation activity to NAD^+ levels in the cell. (Canto and Auwerx 2012, Mouchiroud, Houtkooper et al. 2013, Kupis, Palyga et al. 2016, Zhang and Sauve 2018). Supporters of this hypothesis propose a biochemical justification for this correlation; in some sirtuins such as mammalian SIRT1 and SIRT3, NAD^+ could be the rate limiting substrate due to the Michalis constant (K_M) values near physiological levels in the cell. A summary of the mammalian K_M values can be found in (Katsyuba and Auwerx 2018). Another observation to support this hypothesis is sirtuin compartmentalization. In mammalian cells, sirtuins 1-7 are located in nucleus (1,2,3,6,7), cytoplasm (1,2) and mitochondria (3,4,5). Sirtuins act locally using NAD^+ available in the area (Imai, Johnson et al. 2000), and in some cases such as the mitochondria, NAD^+ is not exchangeable with other organelles. This has led to the hypothesis that sirtuins regulate specific metabolic activities coupled to NAD^+ levels in specific compartments (Zhang and Sauve 2018). While it is clear sirtuins consume NAD^+ for de-acetylation, it is difficult to distinguish if sirtuins are coupled to the metabolic state of the cell or

simply consuming a readily available substrate. Reported physiological levels of NAD^+ in mammalian cells range from 0.3 to 0.5 mM (Sauve, Wolberger et al. 2006), yet the range of reported K_M values is broad (13 to 888 μM) (Katsyuba and Auwerx 2018). In addition, tracking NAD^+ levels and fluctuations in different compartments has proven difficult even with advancing technology (Cambronne, Stewart et al. 2016). The hypothesis is intriguing, but requires further investigation.

An alternative hypothesis as to why sirtuins use NAD^+ is to look for uses of the NAD^+-derived product, O-acetyl ADPr. Historically, sirtuins were discovered as histone deacetylase enzymes, forming O-acetyl ADP ribose (Imai, Armstrong et al. 2000). (Tong and Denu 2010) and others have suggested that O-acetyl ADP ribose could be either a signaling molecule or an important substrate for downstream enzymatic reactions. Some enzymes were found to catalyze O-acetyl ADP ribose such as nucleoside diphosphates linked to x (NUDIX) hydrolases (Bessman, Frick et al. 1996), which yield adenosine monophosphate (AMP) and 2- and 3-O-acetylribose-5-phosphate (McLennan 2006). Both ADP-ribosyl hydrolase enzymes (AHR3) (Ono, Kasamatsu et al. 2006) and macrodomain proteins (Kustatscher, Hothorn et al. 2005) hydrolyze O-acetyl ADP ribose, forming acetyl and ADPr. Some evidence was found for O-acetyl ADP ribose as a signaling molecule such as a possible ligand of transient receptor potential cation channel subfamily M member 2 (TRPM2) calcium channels in the plasma membrane (Grubisha, Rafty et al. 2006). O-acetyl ADPr was proposed to assist with silent information regulator (SIR) complex assembly onto nucleosomes in yeast (Liou, Tanny et al. 2005), but this finding was later contradicted by (Chou, Li et al. 2008). Experiments seeking a signaling role for O-acetyl ADPr in eukaryotes are not only inconclusive, but they also fail to

account for the presence of sirtuins in bacteria and archaea that lack putative O-acetyl ADP ribose targets such as TRP channels.

1.5 Substrates of Sirtuins

As the search for downstream pathways and biological relavent use of O-acetyl ADP ribose continued, it was discovered that sirtuins could remove modifications beyond the assumed role of acetylated histones. This meant sirtuins used NAD^+ to synthesize different types of O-acyl ADP ribose (O-acyl ADPr) molecules from NAD^+ (fig1.4). *Salmonella* CobB was the first sirtuin shown to have biologically relevant deacylation activity. CobB regulates propionyl-CoA synthetase by depropionylating an active site lysine allowing the bacterial cell to grow better in propionate (Garrity, Gardner et al. 2007). (Smith and Denu 2007) further discovered that eukaryotic sirtuins could also remove propionyl and butyrl modified groups from peptide lysines creating corresponding O-propionyl and O-butyrl ADP ribose, respectively. When extra density corresponding to a negatively charged buffer molecule interacting with residues Tyr102 and Arg105 in the active site of SIRT5, (Du, Zhou et al. 2011) hypothesized human sirtuin, SIRT5, could remove negatively charged acyl chains. They discovered that not only could SIRT5 remove malonyl and succinyl lysine chains, but that SIRT5 removed these acyl groups preferentially, catalyzing malonyl and succinyl-lysine peptides 29- to 1,000-fold more efficiently than acetyl-lysine. We now know that sirtuins from all three domains of life preferentially remove a variety of acyl lysine modifications such as negatively charged acyl chains (Du, Zhou et al. 2011, Ringel, Roman et al. 2014), long fatty acyl chains (Zhu, Zhou et al. 2012, Feldman, Baeza et al. 2013, Jiang, Khan et al. 2013), lipoyl chains (Mathias, Greco et al. 2014), and 3-

methyl glutaryl (Anderson, Huynh et al. 2017), creating the corresponding O-acyl ADP ribose product (Fig 1.4).

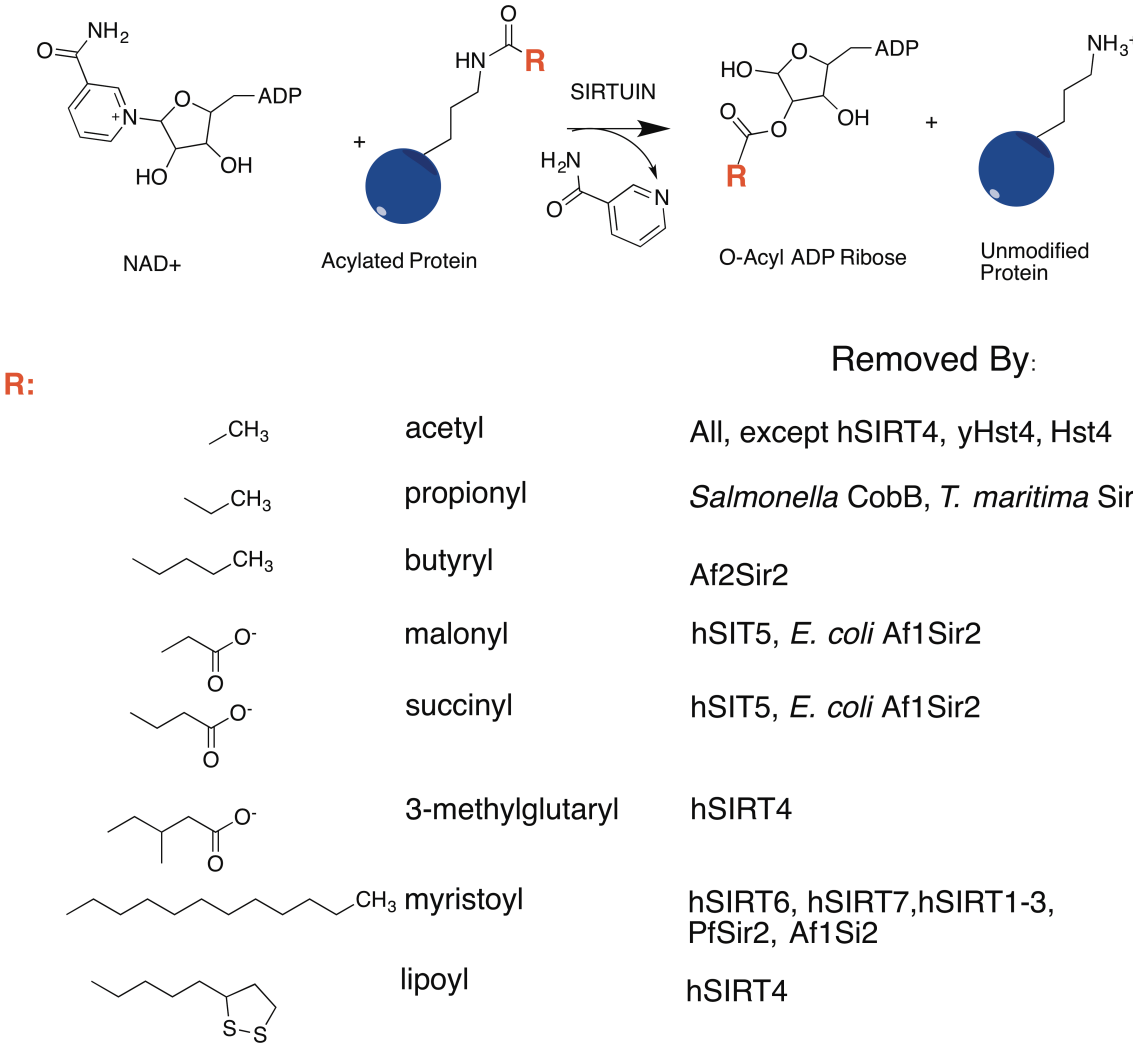

Fig 1.4 Substrates of sirtuins. Sirtuins from all three domain of life preferentially remove a variety of acyl-lysine peptide modifications (depicted by **R**), forming the corresponding O-acyl ADP ribose product.

1.6 Non-enzymatic Acylation and the Hypothesized role of Sirtuins

At the same time, mass spectrometry studies have revealed an abundance of proteins with acyl-lysine modifications in the cell serving as potential sirtuin targets (Chen, Sprung et al. 2007, Cheng, Tang et al. 2009, Zhang, Tan et al. 2011, Colak, Xie et al. 2013, Wagner and Payne 2013, Nishida, Rardin et al. 2015). For example, one study found 2565 succinylation sites on the 779 proteins in mouse liver tissue alone (Park, Chen et al. 2013): It was further hypothesized, and is now commonly accepted, that some acyl lysine modifications occur non-enzymatically (Wagner and Payne 2011, Ghanta, Grossmann et al. 2013, Wagner and Hirschey 2014, Trub and Hirschey 2018). Evidence for non-enzymatic acylation includes the absence of known acyl-transferases for some of these modifications, and the intrinsic reactivity of certain highly reactive metabolite such as acyl-CoAs (Baddiley, Kekwick et al. 1952, Paik, Pearson et al. 1970, d'Alayer, Expert-Bezancon et al. 2007) and acyl-phosphates (Weinert, Iesmantavicius et al. 2013), which are common byproducts of cell metabolism. In general, these acyl modifications inhibit to metabolic enzymes (Ghanta, Grossmann et al. 2013, Rardin, He et al. 2013). For example, lysine acylation could neutralize a positive charge, change hydrogen bonding potential, or cause a protein conformational change all of which could affect protein-protein binding or protein-substrate binding (Shimazu, Hirschey et al. 2010, Bharathi, Zhang et al. 2013). These new discoveries led to a newly hypothesized biological role of sirtuins. The byproducts of metabolism, termed 'carbon stress' react non-enzymatically with proteins causing a decrease in activity; the sirtuin 'cleans up' the carbon stress by removing the acyl chain and placing it on ADP-ribose (fig1.5) (Wagner and Hirschey 2014).

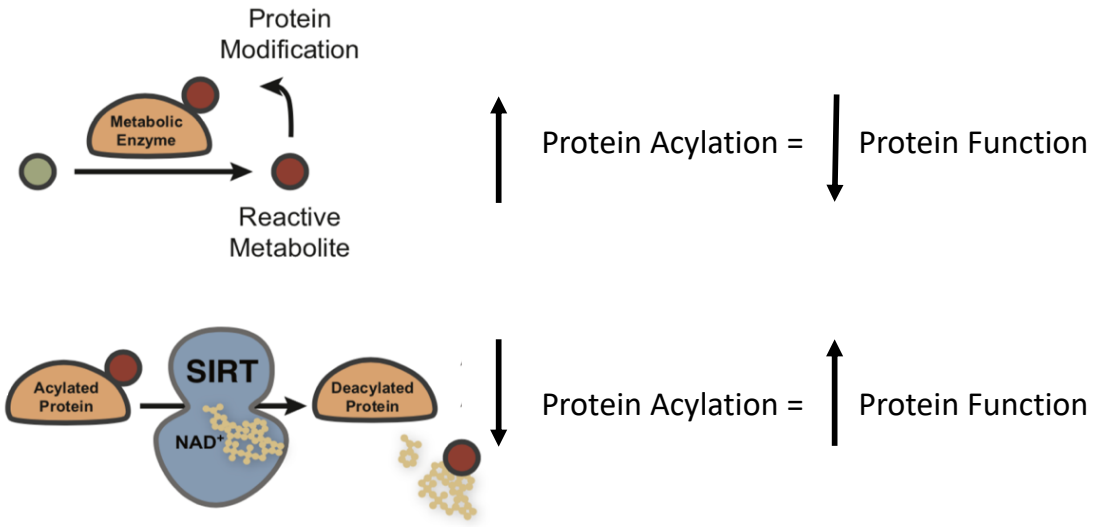

Figure 1.5 Model of sirtuin-mediated protein quality control.

Top: Reactive metabolites or non-enzymatically react with protein lysines forming acyl modifications inhibiting or decreasing protein function that could be considered carbon stress. Bottom: Sirtuins clean up carbon stress by removing acyl modifications which restores protein function. Figure adapted from Wagner and Hirschey 2014)

1.7 Hypothesis: NAD^+ Provides a Nucleotide Carrier to Clean up Carbon Stress

The newly discovered role of sirtuins removing a variety of acyl chains along with its hypothesized role of cleaning up carbon stress to restore protein function leads to the question: what then does the cell do with the acyl chains that are removed from lysine? I hypothesize that sirtuins use NAD^+ to provide a nucleotide carrier, ADP ribose, for the leaving acyl group. Just as acyl groups are transferred to their enzyme substrates from the nucleotide carrier, Coenzyme A (CoA), I hypothesize ADP ribose has a similar role and shuttles acyl chains to enzymes that incorporate it into newly-formed metabolites (Fig 1.6).

1.8 Objectives

In the past three decades since their discovery, sirtuins have been found to play a broad role in many biological processes through deacylation of various protein substrates. The main objective of this work was to test my hypothesis and search for metabolites that incorporated acyl chains carried by O-acyl ADPr and the subsequent enzymes facilitating these reactions. To achieve this, I synthesized O-succinyl ADPr with an isotopically labeled succinyl group, and detected metabolites with that incorporated the isotopic label by mass spectrometry. Specifically, the contributions offered herein are 1) the development of a method for synthesizing and purifying O-succinyl ADP ribose with an isotopically labeled succinyl group, 2) characterization of the natural breakdown and metabolism of O-succinyl ADPr, and 3) an initial metabolomics search for metabolites from the succinyl chain of O-succinyl ADPr.

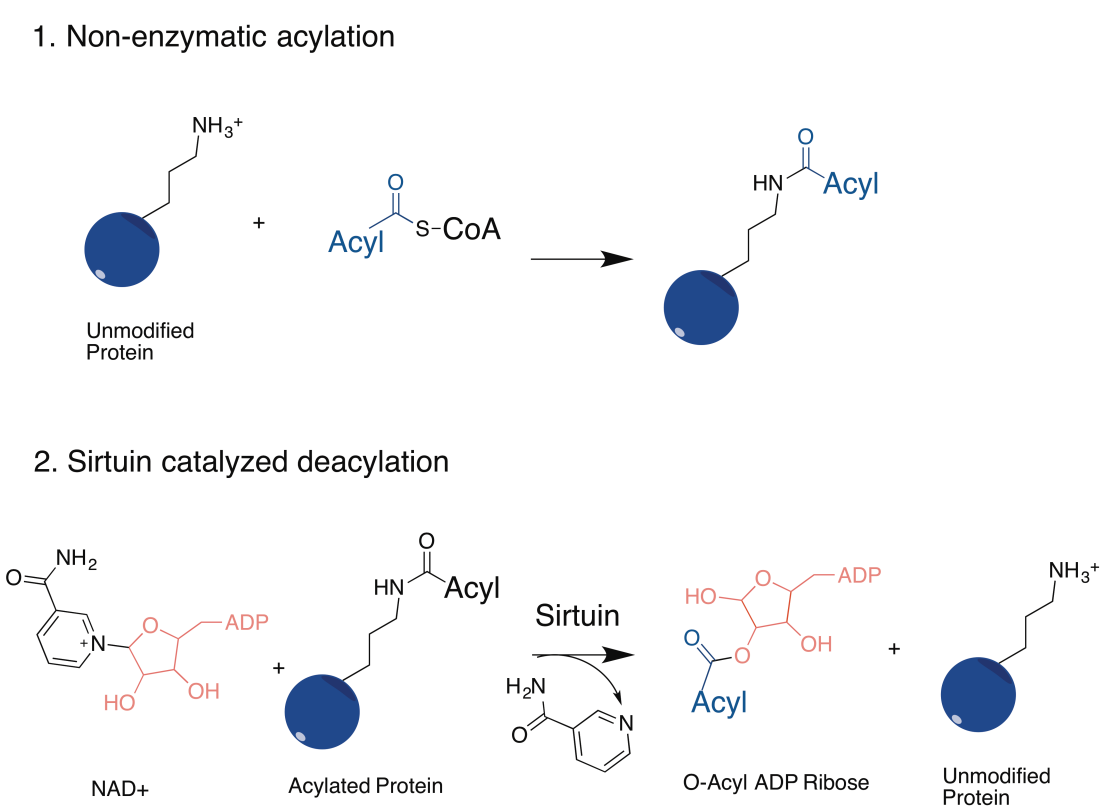

Figure 1.6: Sirtuins provide a carrier molecule to clean up carbon stress. 1. Intrinsically reactive metabolites such as Acyl-CoA react non-enzymatically with protein lysine. 2. Sirtuins remove acyl chains by placing them on the nucleotide carrier, ADP ribose 3. O-acyl ADP ribose shuttles acyl chains into downstream metabolic pathways.

1.9 References

Alageel, A., J. Tomasi, C. Tersigni, E. Brietzke, H. Zuckerman, M. Subramaniapillai, Y. Lee, M. Iacobucci, J. D. Rosenblat, R. B. Mansur and R. S. McIntyre (2018). "Evidence supporting a mechanistic role of sirtuins in mood and metabolic disorders." Prog Neuropsychopharmacol Biol Psychiatry **86**: 95-101.

Anderson, K. A., F. K. Huynh, K. Fisher-Wellman, J. D. Stuart, B. S. Peterson, J. D. Douros, G. R. Wagner, J. W. Thompson, A. S. Madsen, M. F. Green, R. M. Sivley, O. R. Ilkayeva, R. D. Stevens, D. S. Backos, J. A. Capra, C. A. Olsen, J. E. Campbell, D. M. Muoio, P. A. Grimsrud and M. D. Hirschey (2017). "SIRT4 Is a Lysine Deacylase that Controls Leucine Metabolism and Insulin Secretion." Cell Metab **25**(4): 838-855 e815.

Avalos, J. L., I. Celic, S. Muhammad, M. S. Cosgrove, J. D. Boeke and C. Wolberger (2002). "Structure of a Sir2 enzyme bound to an acetylated p53 peptide." Mol Cell **10**(3): 523-535.

Baddiley, J., R. A. Kekwick and E. M. Thain (1952). "A new method for acetylating proteins." Nature **170**(4336): 968-970.

Bessman, M. J., D. N. Frick and S. F. O'Handley (1996). "The MutT proteins or "Nudix" hydrolases, a family of versatile, widely distributed, "housecleaning" enzymes." J Biol Chem **271**(41): 25059-25062.

Bharathi, S. S., Y. Zhang, A. W. Mohsen, R. Uppala, M. Balasubramani, E. Schreiber, G. Uechi, M. E. Beck, M. J. Rardin, J. Vockley, E. Verdin, B. W. Gibson, M. D. Hirschey and E. S. Goetzman (2013). "Sirtuin 3 (SIRT3) protein regulates long-chain acyl-CoA dehydrogenase by deacetylating conserved lysines near the active site." J Biol Chem **288**(47): 33837-33847.

Bheda, P., H. Jing, C. Wolberger and H. Lin (2016). "The Substrate Specificity of Sirtuins." Annu Rev Biochem **85**: 405-429.

Borra, M. T., M. R. Langer, J. T. Slama and J. M. Denu (2004). "Substrate specificity and kinetic mechanism of the Sir2 family of NAD+-dependent histone/protein deacetylases." Biochemistry **43**(30): 9877-9887.

Cambronne, X. A., M. L. Stewart, D. Kim, A. M. Jones-Brunette, R. K. Morgan, D. L. Farrens, M. S. Cohen and R. H. Goodman (2016). "Biosensor reveals multiple sources for mitochondrial NAD(+)." Science **352**(6292): 1474-1477.

Canto, C. and J. Auwerx (2012). "Targeting sirtuin 1 to improve metabolism: all you need is NAD(+)?" Pharmacol Rev **64**(1): 166-187.

Chen, Y., R. Sprung, Y. Tang, H. Ball, B. Sangras, S. C. Kim, J. R. Falck, J. Peng, W. Gu and Y. Zhao (2007). "Lysine propionylation and butyrylation are novel post-translational modifications in histones." Mol Cell Proteomics **6**(5): 812-819.

Cheng, Z., Y. Tang, Y. Chen, S. Kim, H. Liu, S. S. Li, W. Gu and Y. Zhao (2009). "Molecular characterization of propionyllysines in non-histone proteins." Mol Cell Proteomics **8**(1): 45-52.

Chou, C. C., Y. C. Li and M. R. Gartenberg (2008). "Bypassing Sir2 and O-acetyl-ADP-ribose in transcriptional silencing." Mol Cell **31**(5): 650-659.

Colak, G., Z. Xie, A. Y. Zhu, L. Dai, Z. Lu, Y. Zhang, X. Wan, Y. Chen, Y. H. Cha, H. Lin, Y. Zhao and M. Tan (2013). "Identification of lysine succinylation substrates and the succinylation regulatory enzyme CobB in Escherichia coli." Mol Cell Proteomics **12**(12): 3509-3520.

Cosgrove, M. S., K. Bever, J. L. Avalos, S. Muhammad, X. Zhang and C. Wolberger (2006). "The structural basis of sirtuin substrate affinity." Biochemistry **45**(24): 7511-7521.

d'Alayer, J., N. Expert-Bezancon and P. Beguin (2007). "Time- and temperature-dependent acetylation of the chemokine RANTES produced in recombinant Escherichia coli." Protein Expr Purif **55**(1): 9-16.

Du, J., Y. Zhou, X. Su, J. J. Yu, S. Khan, H. Jiang, J. Kim, J. Woo, J. H. Kim, B. H. Choi, B. He, W. Chen, S. Zhang, R. A. Cerione, J. Auwerx, Q. Hao and H. Lin (2011). "Sirt5 is a NAD-dependent protein lysine demalonylase and desuccinylase." Science **334**(6057): 806-809.

Eskandarian, H. A., F. Impens, M. A. Nahori, G. Soubigou, J. Y. Coppee, P. Cossart and M. A. Hamon (2013). "A role for SIRT2-dependent histone H3K18 deacetylation in bacterial infection." Science **341**(6145): 1238858.

Feldman, J. L., J. Baeza and J. M. Denu (2013). "Activation of the protein deacetylase SIRT6 by long-chain fatty acids and widespread deacylation by mammalian sirtuins." J Biol Chem **288**(43): 31350-31356.

Frye, R. A. (2000). "Phylogenetic classification of prokaryotic and eukaryotic Sir2-like proteins." Biochem Biophys Res Commun **273**(2): 793-798.

Garrity, J., J. G. Gardner, W. Hawse, C. Wolberger and J. C. Escalante-Semerena (2007). "N-lysine propionylation controls the activity of propionyl-CoA synthetase." J Biol Chem **282**(41): 30239-30245.

Ghanta, S., R. E. Grossmann and C. Brenner (2013). "Mitochondrial protein acetylation as a cell-intrinsic, evolutionary driver of fat storage: chemical and metabolic logic of acetyl-lysine modifications." Crit Rev Biochem Mol Biol **48**(6): 561-574.

Grubisha, O., L. A. Rafty, C. L. Takanishi, X. Xu, L. Tong, A. L. Perraud, A. M. Scharenberg and J. M. Denu (2006). "Metabolite of SIR2 reaction modulates TRPM2 ion channel." J Biol Chem **281**(20): 14057-14065.

Guarente, L. (2018). Chapter 1 - Sirtuins, NAD+, Aging, and Disease: A Retrospective and Prospective Overview. Introductory Review on Sirtuins in Biology, Aging, and Disease. L. Guarente, R. Mostoslavsky and A. Kazantsev, Academic Press**:** 1-6.

Hoff, K. G., J. L. Avalos, K. Sens and C. Wolberger (2006). "Insights into the sirtuin mechanism from ternary complexes containing NAD+ and acetylated peptide." Structure **14**(8): 1231-1240.

Imai, S., C. M. Armstrong, M. Kaeberlein and L. Guarente (2000). "Transcriptional silencing and longevity protein Sir2 is an NAD-dependent histone deacetylase." Nature **403**(6771): 795-800.

Imai, S., F. B. Johnson, R. A. Marciniak, M. McVey, P. U. Park and L. Guarente (2000). "Sir2: an NAD-dependent histone deacetylase that connects chromatin silencing, metabolism, and aging." Cold Spring Harb Symp Quant Biol **65**: 297-302.

Jiang, H., S. Khan, Y. Wang, G. Charron, B. He, C. Sebastian, J. Du, R. Kim, E. Ge, R. Mostoslavsky, H. C. Hang, Q. Hao and H. Lin (2013). "SIRT6 regulates TNF-alpha secretion through hydrolysis of long-chain fatty acyl lysine." Nature **496**(7443): 110-113.

Kane, A. E. and D. A. Sinclair (2018). Chapter 6 - Pharmacological Approaches for Modulating Sirtuins. Introductory Review on Sirtuins in Biology, Aging, and Disease. L. Guarente, R. Mostoslavsky and A. Kazantsev, Academic Press**:** 71-81.

Katsyuba, E. and J. Auwerx (2018). Chapter 3 - NAD+ Modulation: Biology and Therapy. Introductory Review on Sirtuins in Biology, Aging, and Disease. L. Guarente, R. Mostoslavsky and A. Kazantsev, Academic Press**:** 27-44.

Kupis, W., J. Palyga, E. Tomal and E. Niewiadomska (2016). "The role of sirtuins in cellular homeostasis." J Physiol Biochem **72**(3): 371-380.

Kustatscher, G., M. Hothorn, C. Pugieux, K. Scheffzek and A. G. Ladurner (2005). "Splicing regulates NAD metabolite binding to histone macroH2A." Nat Struct Mol Biol **12**(7): 624-625.

Liou, G. G., J. C. Tanny, R. G. Kruger, T. Walz and D. Moazed (2005). "Assembly of the SIR complex and its regulation by O-acetyl-ADP-ribose, a product of NAD-dependent histone deacetylation." Cell **121**(4): 515-527.

Ma, L. and Y. Li (2015). "SIRT1: Role in cardiovascular biology." Clinica Chimica Acta **440**: 8-15.

Mathias, R. A., T. M. Greco, A. Oberstein, H. G. Budayeva, R. Chakrabarti, E. A. Rowland, Y. Kang, T. Shenk and I. M. Cristea (2014). "Sirtuin 4 is a lipoamidase regulating pyruvate dehydrogenase complex activity." Cell **159**(7): 1615-1625.

McLennan, A. G. (2006). "The Nudix hydrolase superfamily." Cell Mol Life Sci **63**(2): 123-143.

Mouchiroud, L., R. H. Houtkooper and J. Auwerx (2013). "NAD(+) metabolism: a therapeutic target for age-related metabolic disease." Crit Rev Biochem Mol Biol **48**(4): 397-408.

Nishida, Y., M. J. Rardin, C. Carrico, W. He, A. K. Sahu, P. Gut, R. Najjar, M. Fitch, M. Hellerstein, B. W. Gibson and E. Verdin (2015). "SIRT5 Regulates both Cytosolic and Mitochondrial Protein Malonylation with Glycolysis as a Major Target." Mol Cell **59**(2): 321-332.

Ono, T., A. Kasamatsu, S. Oka and J. Moss (2006). "The 39-kDa poly(ADP-ribose) glycohydrolase ARH3 hydrolyzes O-acetyl-ADP-ribose, a product of the Sir2 family of acetyl-histone deacetylases." Proc Natl Acad Sci U S A **103**(45): 16687-16691.

Paik, W. K., D. Pearson, H. W. Lee and S. Kim (1970). "Nonenzymatic acetylation of histones with acetyl-CoA." Biochim Biophys Acta **213**(2): 513-522.

Park, J., Y. Chen, Daniel X. Tishkoff, C. Peng, M. Tan, L. Dai, Z. Xie, Y. Zhang, Bernadette M. M. Zwaans, Mary E. Skinner, David B. Lombard and Y. Zhao (2013). "SIRT5-Mediated Lysine Desuccinylation Impacts Diverse Metabolic Pathways." Molecular Cell **50**(6): 919-930.

Pinzone, M. R., B. Cacopardo, F. Condorelli, M. Di Rosa and G. Nunnari (2013). "Sirtuin-1 and HIV-1: an overview." Curr Drug Targets **14**(6): 648-652.

Rardin, M. J., W. He, Y. Nishida, J. C. Newman, C. Carrico, S. R. Danielson, A. Guo, P. Gut, A. K. Sahu, B. Li, R. Uppala, M. Fitch, T. Riiff, L. Zhu, J. Zhou, D. Mulhern, R. D. Stevens, O. R. Ilkayeva, C. B. Newgard, M. P. Jacobson, M. Hellerstein, E. S. Goetzman, B. W. Gibson and E. Verdin (2013). "SIRT5 regulates the mitochondrial lysine succinylome and metabolic networks." Cell Metab **18**(6): 920-933.

Reed, N. A., D. Cai, T. L. Blasius, G. T. Jih, E. Meyhofer, J. Gaertig and K. J. Verhey (2006). "Microtubule acetylation promotes kinesin-1 binding and transport." Curr Biol **16**(21): 2166-2172.

Ringel, A. E., C. Roman and C. Wolberger (2014). "Alternate deacylating specificities of the archaeal sirtuins Sir2Af1 and Sir2Af2." Protein Sci **23**(12): 1686-1697.

Rossmann, M. G. and P. Argos (1978). "The taxonomy of binding sites in proteins." Mol Cell Biochem **21**(3): 161-182.

Sauve, A. A., C. Wolberger, V. L. Schramm and J. D. Boeke (2006). "The biochemistry of sirtuins." Annu Rev Biochem **75**: 435-465.

Sebastian, C., F. K. Satterstrom, M. C. Haigis and R. Mostoslavsky (2012). "From sirtuin biology to human diseases: an update." J Biol Chem **287**(51): 42444-42452.

Shimazu, T., M. D. Hirschey, L. Hua, K. E. Dittenhafer-Reed, B. Schwer, D. B. Lombard, Y. Li, J. Bunkenborg, F. W. Alt, J. M. Denu, M. P. Jacobson and E. Verdin (2010). "SIRT3 deacetylates mitochondrial 3-hydroxy-3-methylglutaryl CoA synthase 2 and regulates ketone body production." Cell Metab **12**(6): 654-661.

Shore, D., M. Squire and K. A. Nasmyth (1984). "Characterization of two genes required for the position-effect control of yeast mating-type genes." EMBO J **3**(12): 2817-2823.

Smith, B. C. and J. M. Denu (2007). "Acetyl-lysine analog peptides as mechanistic probes of protein deacetylases." J Biol Chem **282**(51): 37256-37265.

Szegő, É. M., T. F. Outeiro and A. G. Kazantsev (2018). Chapter 13 - Sirtuins in Brain and Neurodegenerative Disease. Introductory Review on Sirtuins in Biology, Aging, and Disease. L. Guarente, R. Mostoslavsky and A. Kazantsev, Academic Press**:** 175-195.

Tong, L. and J. M. Denu (2010). "Function and metabolism of sirtuin metabolite O-acetyl-ADP-ribose." Biochim Biophys Acta **1804**(8): 1617-1625.

Trub, A. G. and M. D. Hirschey (2018). "Reactive Acyl-CoA Species Modify Proteins and Induce Carbon Stress." Trends Biochem Sci **43**(5): 369-379.

Vachharajani, V. T., T. Liu, X. Wang, J. J. Hoth, B. K. Yoza and C. E. McCall (2016). "Sirtuins Link Inflammation and Metabolism." J Immunol Res **2016**: 8167273.

Wagner, G. R. and M. D. Hirschey (2014). "Nonenzymatic protein acylation as a carbon stress regulated by sirtuin deacylases." Mol Cell **54**(1): 5-16.

Wagner, G. R. and R. M. Payne (2011). "Mitochondrial acetylation and diseases of aging." J Aging Res **2011**: 234875.

Wagner, G. R. and R. M. Payne (2013). "Widespread and enzyme-independent Nepsilon-acetylation and Nepsilon-succinylation of proteins in the chemical conditions of the mitochondrial matrix." J Biol Chem **288**(40): 29036-29045.

Weinert, B. T., V. Iesmantavicius, S. A. Wagner, C. Scholz, B. Gummesson, P. Beli, T. Nystrom and C. Choudhary (2013). "Acetyl-phosphate is a critical determinant of lysine acetylation in E. coli." Mol Cell **51**(2): 265-272.

Xiong, S., G. Salazar, N. Patrushev and R. W. Alexander (2011). "FoxO1 mediates an autofeedback loop regulating SIRT1 expression." J Biol Chem **286**(7): 5289-5299.

Zhang, N. and A. A. Sauve (2018). Chapter Three - Regulatory Effects of NAD+ Metabolic Pathways on Sirtuin Activity. Progress in Molecular Biology and Translational Science. W. Zheng, Academic Press. **154:** 71-104.

Zhang, Z., M. Tan, Z. Xie, L. Dai, Y. Chen and Y. Zhao (2011). "Identification of lysine succinylation as a new post-translational modification." Nat Chem Biol **7**(1): 58-63.

Zhu, A. Y., Y. Zhou, S. Khan, K. W. Deitsch, Q. Hao and H. Lin (2012). "Plasmodium falciparum Sir2A preferentially hydrolyzes medium and long chain fatty acyl lysine." ACS Chem Biol **7**(1): 155-159.

Chapter 2

Synthesis and Purification of ^{13}C-labeled O-succinyl ADP ribose

2.1 Introduction

Sirtuins are an ancient family of enzymes all defined by their 250 amino acid core residues. Analysis of sirtuin protein sequences and structures suggested that this family of enzymes was found in the last universal common ancestor (LUCA) due to its conserved Rossman fold and NAD-binding domain (Aravind, Mazumder et al. 2002). Phylogenic analysis has suggested that sirtuins have diversified greatly (Frye 2000, Iyer, Anantharaman et al. 2008). They are divided into distinct classes and further subclasses (Frye 2000, Hirschey, Shimazu et al. 2011). Often sirtuins within these classes remove a specific type of acyl modification, and in higher level organisms they are compartmentalized in the same organelles. For example, sirtuins in class III are located in the mitochondria and remove negatively charged acyl chains. Their phylogenic diversification and preferential deacylation activity presented a challenge for choosing a model sirtuin and organism to search for an evolutionarily conserved downstream metabolic pathway.

To address this challenge, I considered several factors: the model organism, the class of sirtuin and the specific acyl modification. *E. coli* is a favored model organism to study metabolism for many obvious reasons including its relatively simple, well-documented genome and straightforward growth conditions. It has the advantage of having a free metabolomic database, the *E. coli* metabolome database (ECMDB), containing currently 1542 known metabolic pathways (http://ecmdb.ca). ECMDB can be used to either rule out a newly discovered pathway or connect a discovered pathway to a larger, known metabolic pathway. Using *E. coli* has the additional advantage of grouping genes in operons, a cluster of genes under the same

promotor that often function in the same process. *E. coli* operons could be used to fully describe all proteins in a metabolic pathway. Others have found NAD-utilizing metabolic pathways using operons as a guide (de Souza and Aravind 2012).

E. coli has one sirtuin, CobB, from phylogenic class III of the sirtuin family. Class III sirtuins are found in all archaea, bacteria, and lower and higher level eukaryotes (Frye 2000). It is the most widely distributed sirtuin of all of the classes and is predicted to be the most ancient of the sirtuins (Frye 2000). Like all members of this family, CobB preferentially removes negatively charged acyl chains such as malonyl and succinyl lysine (Ringel, Roman et al. 2014). I chose to study the succinyl chain as a model acyl modification that is carried on ADPr. As with the class III sirtuins, succinylation is found widely spread across organisms in all three domains of life (Zhang, Tan et al. 2011, Park, Chen et al. 2013) making the succinyl group on O-succinyl ADPr a hopeful target model acyl group to use to search for downstream metabolic pathways.

In order to follow the fate of the succinyl chain on O-succinyl ADPr in *E. coli* cell lysates, I needed a synthesis method of O-succinyl ADPr that allowed for isotopic labeling of the succinyl group (Fig. 2.1). Previous methods to synthesize O-acyl ADPr molecules both chemically (Szczepankiewicz, Koppetsch et al. 2011) and enzymatically (Jackson and Denu 2002) exist in the literature. Chemical synthesis involves a simple one-step

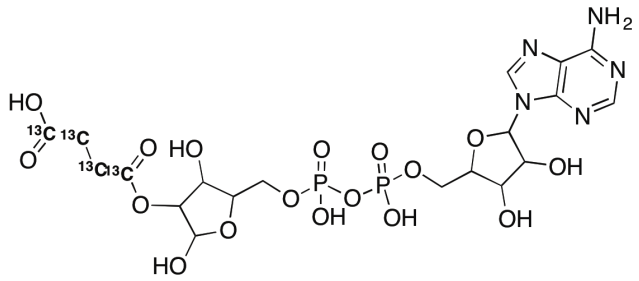

Figure 2.1 ^{13}C-labeled O-succinyl ADP Ribose. The acyl chain is isotopically labeled with ^{13}C, so upon incubation with *E. coli* cell lysates, metabolites incorporating the succinyl group can be identified by mass spectrometry.

reaction with NAD^+, sodium acetate and acetic acid; the disadvantage of this method is that the reaction yield decreases as the size of the acyl chain increases. Enzymatic synthesis is a common method for the making O-acetyl ADPr; (Jackson and Denu 2002) pioneered this method by treating acetylated lysine peptides with a sirtuin. Many have enzymatically synthesized isotopically labeled O-acetyl ADPr with a ^{14}C-label on the ADPr portion of the molecule, but the literature has not reported an O-acyl ADPr molecule with an isotopic label on the acyl chain. However, it is well known that treatment of lysine peptides with acyl anhydrides is an efficient and common reaction that yields acylated-lysine peptides (Aitken and Learmonth 1996, Bheda, Swatkoski et al. 2012). Acyl anhydrides are inexpensive and come with a variety of isoptopic labels, allowing for the synthesis of a variety of labeling options for isotopic succinyl lysine (Sigma 578517, 603902). Treatment of that isotopic succinyl peptide with a sirtuin will result in an isotopically labeled O-succinyl ADPr molecule. In this chapter, I present an adaption of (Jackson and Denu 2002)'s method for enzymatic synthesis of O-succinyl ADPr which proceeds in 2 steps chemical succinylation of lysines using succinic anhydride, and enzymatic desuccinylation of lysines catalyzed by a sirtuin with the cofactor NAD^+ (Fig. 2.2). I succinylated histone H2B, which has 20 potentially accessible lysines available for modification and found a 50 to 1 ratio of anhydride to histone H2B resulted in full succinylation of lysines. Interestingly, I found I could not adapt Jackson and Denu's HPLC purification protocol for O-acetyl ADPr to O-succinyl ADPr, possibly due to the extra polarity from the carbonyl oxygen and came up with a novel HPLC purification method detailed below. Finally, I show ^1H NMR and mass spectrometry data verifying synthesis and purity of both unlabeled and ^{13}C-labeled O-succinyl ADPr.

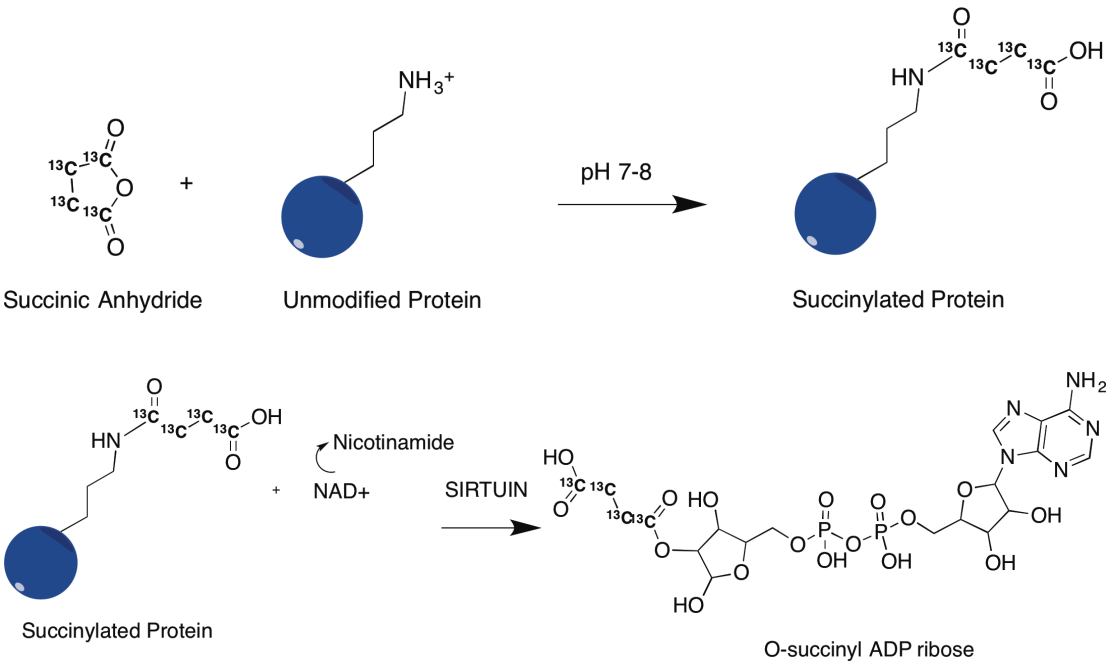

Figure 2.2 Synthesis method of O-succinyl ADPr. (Top) Chemical succinylation by treatment of unmodified lysine protein with ^{13}C-labeled succinic anhydride. (Bottom) Enzymatic desuccinylation of succinylated lysine protein with sirtuin and NAD^+.

2.2 Methods

Chemical Succinylation of Histone H2B

Purified histone H2B was provided by Mike Morgan and prepared as described (Luger, Rechsteiner et al. 1999). 150 μM lyophilized histone H2B was brought up in 200 mM sodium borate, pH 8. Succinic anhydride was added incrementally to a final concentration of 150 mM. The solution was kept at stirring at room temperature, pH 7.0 to 9.0. Once fully mixed, the reaction was allowed to proceed to completion for 30 minutes on ice where it was immediately washed with MilliQ water on a desalting column (PD-10, GE) and dialyzed in 4L of MilliQ water overnight.

SIRT5 Growth and Purification

SIRT5-pET-15b (Addgene plasmid # 81030) was expressed and purified as described previously (Hallows, Lee et al. 2006). Briefly, the plasmid was transformed into Rosetta2-(DE3) *E. coli* cells (EMD Millipore) and grown overnight in at 37°C in 2xYT containing 50 μg/ml kanamycin and 34 μg/ml chloramphenicol. The saturated cultures were diluted 100-fold into 6 liters of 2x YT media and grown to an OD_{600} of 0.6-0.8. The cultures were cooled on ice for 30 minutes, induced with 0.5 mM IPTG, and grown for an additional 8 hours at 25°C. Cells were harvested by centrifugation and lysed with a microfluidizer (Microfluidics Corp) in 5mM imidazole, 1mM BME, 50mM Tris HCl pH 8, and 250mM NaCl. Cell debris was removed by centrifugation at 32,000 g. Clarified lysate was loaded onto a HisTrap HP column (GE LifeSciences) equilibrated in lysis buffer and eluted with a 5 to 400 mM imidazole gradient over 30 column volumes. Sample was dialyzed in 25 mM Tris (pH 7.5), 100 mM NaCl, 10% glycerol (wt/vol), and 5 mM DTT and stored at -80°C.

SIRT5 Activity Assay

SIRT5 activity was assessed using the Fluor de Lys SIRT5 fluorometric drug discovery kit (Enzo Life Sciences BML-AK413) according to manufacturer's instructions. Briefly, the provided SIRT5 control and prepared SIRT5 at 6 nM, 100 nM, 500 nM and 1 μM concentrations were added to 10 μM Fluor de Lys substrate, 1mM NAD^+, and kit assay buffer. The reaction was initiated by addition of Fluor de Lys substrate, incubated for 1 hour at 37°C, and quenched with developer. Fluorescence was measured in a 100 μl quartz cuvette on a Fluorolog-3 Spectrofluorometer (Horiba) with excitation at 360 nm and emission range collected at 440 nm.

Characterization of Succinylated Histone H2B by MALDI-TOF

Succinylation of histone H2B was verified at the Johns Hopkins Mass Spectrometry and Proteomics Facility on a MALDI-TOF Voyager DE-STR MS (Applied Biosystems). 1μM samples and standards (Protea, PS-142, PS-124, PS-122) were spotted in MALDI matrix, which was prepared with 10mg/ml sinapic acid (Sigma, 85429) in 50% HPLC grade acetonitrile (Fischer Scientific) and 0.1% trifluoroacetic acid (Sigma-302031). Data were collected in reflector mode and analyzed with the Data Explorer software (version 4.8, Applied Biosystems).

Enzymatic Synthesis of O-succinyl ADPr

200 μM succinylated histone H2B was added to 50 μM SIRT5 in 50 mM Tris HCl, pH 8, 137 mM NaCl, 2.7 mM KCl, 1 mM $MgCl_2$, and 1 mg/ml BSA (Sigma 05470). Reaction was initiated with 2 mM NAD^+ (Sigma N7004) and incubated at 37°C for 1 hour. NAD^+-consumption was monitored by a G6DP-enzyme coupled assay as described (Avalos, Celic et al. 2002).

Liquid Chromatography - Mass Spectrometry

Following enzymatic synthesis, samples were quenched with 4x cold methanol, vortexed, and placed on ice for 10 minutes. Following this, samples were spun at 18,000*g* at 4°C for 15 minutes, and the supernatant was extracted and lyophilized. The lyophilized supernatant was reconstituted in 40% acetonitrile in 10 mM ammonium acetate, pH 4.5 and analyzed by liquid chromatography-mass spectrometry (LC-MS). O-succinyl ADPr was injected onto a Dionex Ultimate 3000 μHPLC coupled to a Q-Exactive Orbitrap mass spectrometer (Thermo Scientific) and resolved with a PolyHydroxyethyl A, HILIC column (300 Å, 200 x 2.1mm, PolyLC Inc, Nest group). A gradient of 10 mM ammonium acetate, pH 4.5 (mobile A) and acetonitrile (mobile B) was used. Mass spectrometer was run in full-MS acquisition in negative ion mode. The mass spectrometer parameters were optimized using a direct infusion of ≈ 0.01 M O-succinyl ADPr in 50% acetonitrile with a flow of 0.4 ml/min. The electrospray ionization source parameters were set as follows: sheath gas flow rate 9, Spray voltage 3.2 kV, capillary temperature 320 °C, probe temperature 300 °C, auxiliary gas 0, auxiliary gas heater temperature 30 °C, collision energy 0 eV. Analysis was performed on Xcalibur Qual browser software.

HPLC Purification of O-succinyl ADPr

Following enzymatic synthesis, samples were quenched with 150 μM TFA, vortexed and placed on ice for 10 minutes. Following this, samples were and spun at 18,000*g* at 4°C for 15 minutes. The supernatant was purified by HPLC on a 5 AQ-C18 column (100 Å, 150 x 211.2 mm, ACE) using a 20-100% gradient (0.01% TFA for “Mobile A” and 0.05% TFA in 100% acetonitrile for “Mobile B”). Fractions were lyophilized and frozen in liquid nitrogen for storage at -80 °C

^{1}H-NMR

^{1}H NMR spectra were obtained at the Johns Hopkins Biomolecular NMR facility on a 600 MHz spectrometer (Bruker Avance) at 25 °C. Lyophilized O-succinyl ADPr were reconstituted in 100% D_2O to a concentration of ≈ 100 mM.

2.3 Results

Succinylation of Histone H2B

In order to follow the fate of the succinyl group on O-succinyl ADPr in E. *coli* cell lysates in future experiments, I required a synthesis method for O-succinyl ADPr allowing for isotopic labeling of the acyl group. Previous methods to both chemically (Szczepankiewicz, Koppetsch et al. 2011) and enzymatically (Jackson and Denu 2002) synthesize O-acyl ADPr exist. Previous labeling methods in the literature isotopically labeled the ADPr portion of the molecule, but there are no published methods labeling the acyl chain. Enzymatic synthesis can be used to label the acyl chain. As outlined in figure 2.2, enzymatic synthesis of O-succinyl ADPr occurs in two steps: succinylation of the ε-nitrogen of a lysine side chain by treatment with succinic anhydride, followed by desuccinylation of the modified lysine by a sirtuin and cosubstrate NAD^+.

Treatment of lysine substrates with acyl anhydrides is extremely efficient and has been previously done in our lab (Bheda, Swatkoski et al. 2012). This method allowed me to use both unlabeled and ^{13}C-labeled succinic anhydride (Sigma 578517) to create O-succinyl ADPr with and without an isotopic label. Sigma also sells succinic anhydride-1,4-$^{13}C_2$ (603902) and

succinic anhydride-2-^{13}C which can be used to synthesize the corresponding O-succinyl ADPr's as well.

In order to maximize yield of O-succinyl ADPr, I used recombinant histone H2B as a substrate, which has 20 potential lysine modification sites (Luger, Rechsteiner et al. 1999). As recommended by (Bheda, Swatkoski et al. 2012) and (Aitken and Learmonth 1996), 50x molar excess anhydride was added to lysine. Succinylation of H2B was verified by MALDI-MS. As shown in Figure 2.3, treatment with 50x succinic anhydride shifted the average *m/z* peak of histone H2B (molecular weight of 13,493 Da) by 2000 Da (13,489 m/z to 15,506 m/z). The mass peak is broad due to a non-homogenous mixture of modifications. Each succinyl modification is 100 Da suggesting that on average all 20 lysines were modified. Later, to save material, I reacted 30x molar excess anhydride to lysine and saw the same mass shift by MALDI-MS.

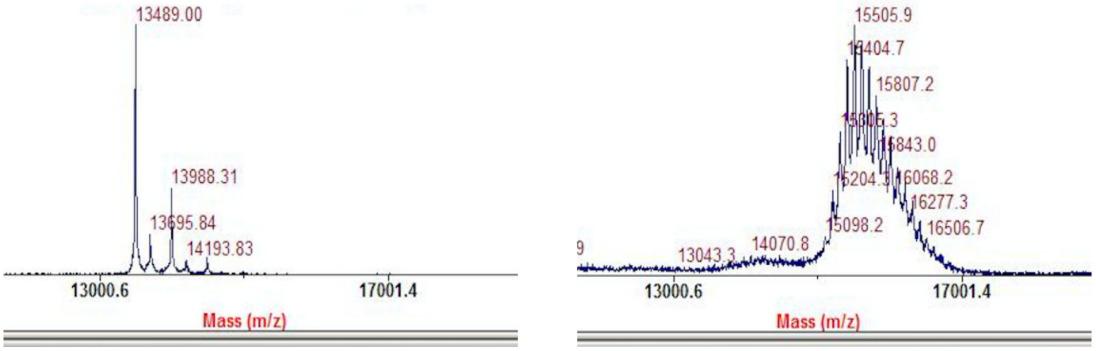

Figure 2.3 MALDI-TOF spectra of (left) unmodified and (right) succinylated histone H2B. Left: Unmodified histone H2B. Theoretical *m/z*: 13,489 experimental *m/z:* 13,493. **Right:** non-homogeneous mixture of histone H2B following treatment with 50:1 molar ratio succinic anhydride. The average experimental *m/z* of modified H2B is 15,506 *m/z*, suggesting a mass shift of 20 succinyl groups where each succinyl group is 100 Da.

Activity of Sirtuins and Synthesis of O-succinyl ADPr

Class III of sirtuins have a conserved tyrosine and arginine residues in the active site, and consequently, remove negatively charged acyl chains 1000-fold more efficiently compared to acetyl-lysine (Du, Zhou et al. 2011). I chose to use two sirtuins from this class of enzymes, CobB and SIRT5 and tested for activity via the Fluro-de-lys ™ enzyme activity assay. As diagramed in Figure 2.4 C, this assay contains a coumarin covalently modified succinyl lysine substrate where upon desuccinylation by a sirtuin becomes accessible to a trypsin developer and produces a fluorometric signal. Using this assay, I discovered I required 1 μM of purified CobB to detect desuccinylation (not shown). However, my purified SIRT5 was more active than CobB with the Fluor-de-lys substrate, and I proceeded using SIRT5. As shown in figure 2.4D, 6 nM, 100 nM, 500 nM and 1 μM were active when incubated with Fluor-de-lys substrate. Due to high abundence of SIRT5 during purification (Fig 2.4 A and B), I decided to proceed using 1 μM to enzyme to ensure maximum yield of O-succinyl ADPr.

To ensure SIRT5 was active on our succinylated histones, I analyzed desuccinylation by MALDI-TOF. Unfortunately, due to the non-homogenous mixture of desuccinylated substrate with varying degrees of desuccinylation, most of the MALDI-MS data had low/signal noise ratio and was difficult to interpret (not shown). Instead, I opted for a simple and more time efficient enzyme-coupled assay to measure the amount of reacted NAD^+ (Avalos, Celic et al. 2002). Briefly, a known amount of NAD^+ is added to sirtuin and modified substrate where it runs until quenched with TFA. A sample of the quenched reaction is added to G6PD which converts all unreacted NAD^+ to NADH which can then be measured spectrophotometrically at an absorbance of 340nm. Since NAD^+ is converted to O-succinyl ADPr in a 1:1 molar ratio, the amount of O-

succinyl ADPr formed can be calculated. Using this method, I verified SIRT5 was active with succinylated histone H2B substrate.

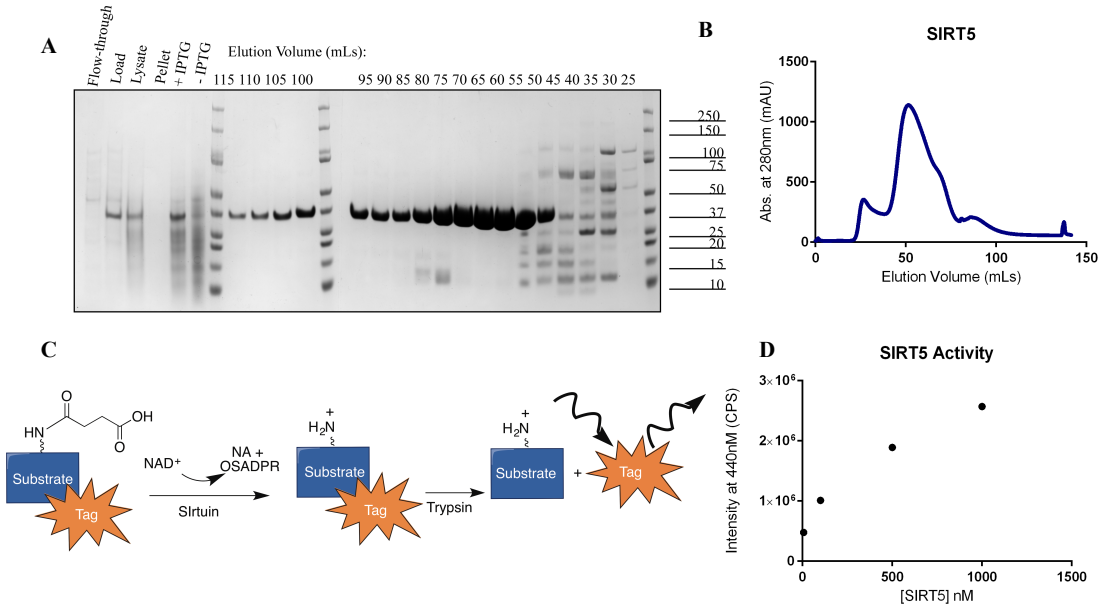

Figure 2.4 Purification and activity of SIRT5. (A) SDS-PAGE gel of growth profile including: pre (-IPTG) and post (+IPTG) induction, pellet and lysate post lysis, load and flow-through onto nickel column. (B) Elution profile of SIRT5 over nickel column. (C) Schematic of Fluor-de Lys activity assay. Tagged acyl substrate upon incubation with sirtuin becomes accessible to a trypsin developer which can be detected fluorometrically. (D) SIRT5 activity profile using fluor-de lys activity assay.

Detection of O-succinyl ADPr by LC-MS

Although I had verified succinylation of H2B by MALDI-TOF and enzymatic synthesis of O-succinyl ADPr by detecting the amount of NAD^+ used, I had not actually detected O-succinyl ADPr. To solve this, I developed a method in collaboration with Dr. Namandje Bumpus and Ms. Carley Heck to detect O-succinyl ADPr by LC-MS. Due to the lack of commercial standard of O-succinyl ADPr available, we optimized MS parameters based on previously published methods (Lee, Tong et al. 2008). These authors previously developed LC-MS methods for detecting O-acetyl ADPr, and we used the column suggested by them (300 Å, 200 x 2.1mm, PolyLC Inc, Nest group). Due to the chemical similarity, we initially optimized mass spectrometry parameters to a standard solution of NAD^+. Following this, succinylated H2B was incubated with SIRT5 in the presence NAD^+ at 37°C for 1 hour, products were methanol extracted and analyzed by LC-MS. As shown in Figure 2.5B, we detected a mass peak of 658.0815 *m/z* corresponding to the exact mass of O-succinyl ADPr (658.0804 *m/z* $\pm$ 2ppm). The corresponding extracted ion chromatogram (Fig. 2.5A) showed a double peak spanning over the retention time of 12 to 14 minutes. Others had observed this double peak and confirmed that O-acetyl ADPr undergoes a sirtuin independent transesterification, equilibrating the 2' and 3' O-acetyl ADPr species (Sauve, Celic et al. 2001, Jackson and Denu 2002). Following this, we ran an identical experiment with ^{13}C-labeled succinic anhydride and detected a mass peak of 662.0946 *m/z* (Figure 2.5D) corresponding to the exact mass of O-succinyl ADPr with the isotopic label (662.0938 *m/z* $\pm$ 2ppm). Figure 2.5C shows the corresponding double peak in the extracted ion chromatogram which matches the retention time and of the unlabeled extracted ion chromatogram.

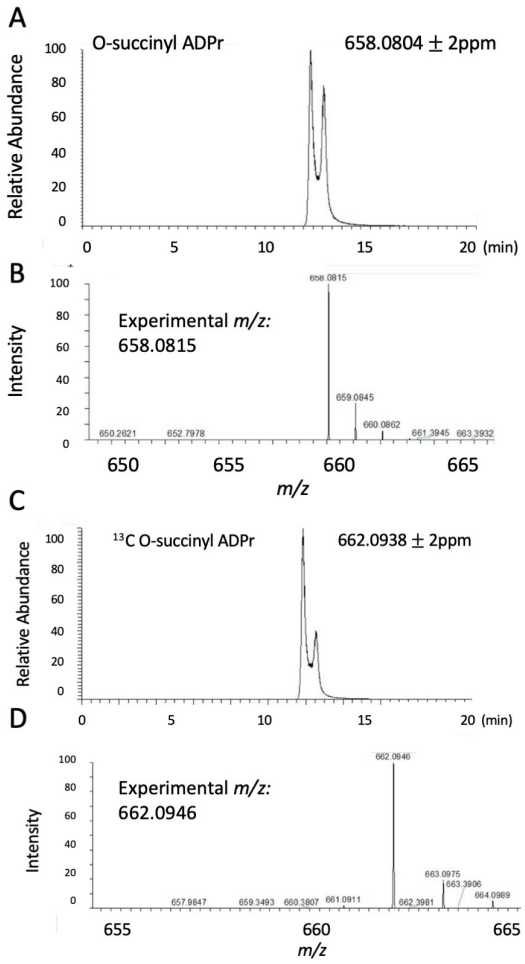

Figure 2.5 Extracted ion chromatogram and mass spectra of unlabeled and ^{13}C O-succinyl ADPr. Product corresponding to O-succinyl ADPr obtained following incubation of NAD^+, succinylated histone H2B and SIRT5. Extracted ion chromatogram (A) and mass spectra corresponding to unlabeled O-succinyl ADPr (B) (theoretical m/z: 658.0804 experimental *m/z:* 658.0815 mass error: 1.7 ppm). Extracted ion chromatogram (C) and mass spectra corresponding to labeled O-succinyl ADPr four ^{13}C-labeled carbons (D) (theoretical m/z: 662.0938 experimental *m/z:* 662.0946 mass error: 1.2ppm)

HPLC Purification and Large-Scale Synthesis of O-succinyl ADPr

After optimizing synthesis of O-succinyl ADPr and verifying its presence, I sought to adapt Denu and Jackson's HPLC purification method for O-succinyl ADPr (Jackson and Denu 2002). There were two challenges to purification: separating NAD^+ from O-succinyl ADPr, and purifying preparative quantities of metabolite. I initially tried our in-house C18 columns as recommended by (Jackson and Denu 2002), but these columns could not separate O-succinyl ADPr from NAD^+. The purification from NAD^+ was important for correctly dosing only O-succinyl ADPr into cell lysates in the later the metabolomics experiment. As shown in Figure 2.6 A, the polar molecules were not retained by the Dynamax C18 (250 x 10 mm) column. Fractions were selected from retention time 5-10 minutes and verified as a mixture of NAD^+ and O-succinyl ADPr by LC-MS (not shown). As shown in Figure 2.6 B, the Kinetex 2.6u XB C18 (275 x 24.6 mm) column also did not retain the injected sample. Fractions at retention time 4-5 minutes contained the mixtures of NAD^+ and O-succinyl ADPr. I attempted to improve retention with both columns by varying method conditions such mobile phase solution gradient before switching to a different column. The ACE 5AQ C18 (150 x 211.2 mm) reverse phase column, which contains proprietary residues to assist with retention of polar small molecules, could retain O-succinyl ADPr and separate it from NAD^+. This column is also designed to purify 10 to 20 mgs of small molecules, so it could handle larger scale preparations if needed. Figure 2.6C is an example chromatogram of the four separate peaks obtained using the ACE 5 AQ C18 column. The chromatogram peaks were identified by LC-MS as adenosine monophosphate (AMP), ADPr, O-succinyl ADPr, and NAD^+ (Fig 2.6 D). It is uncertain where AMP and ADPr came from since they could be degradation products of either O-succinyl ADPr or NAD^+.

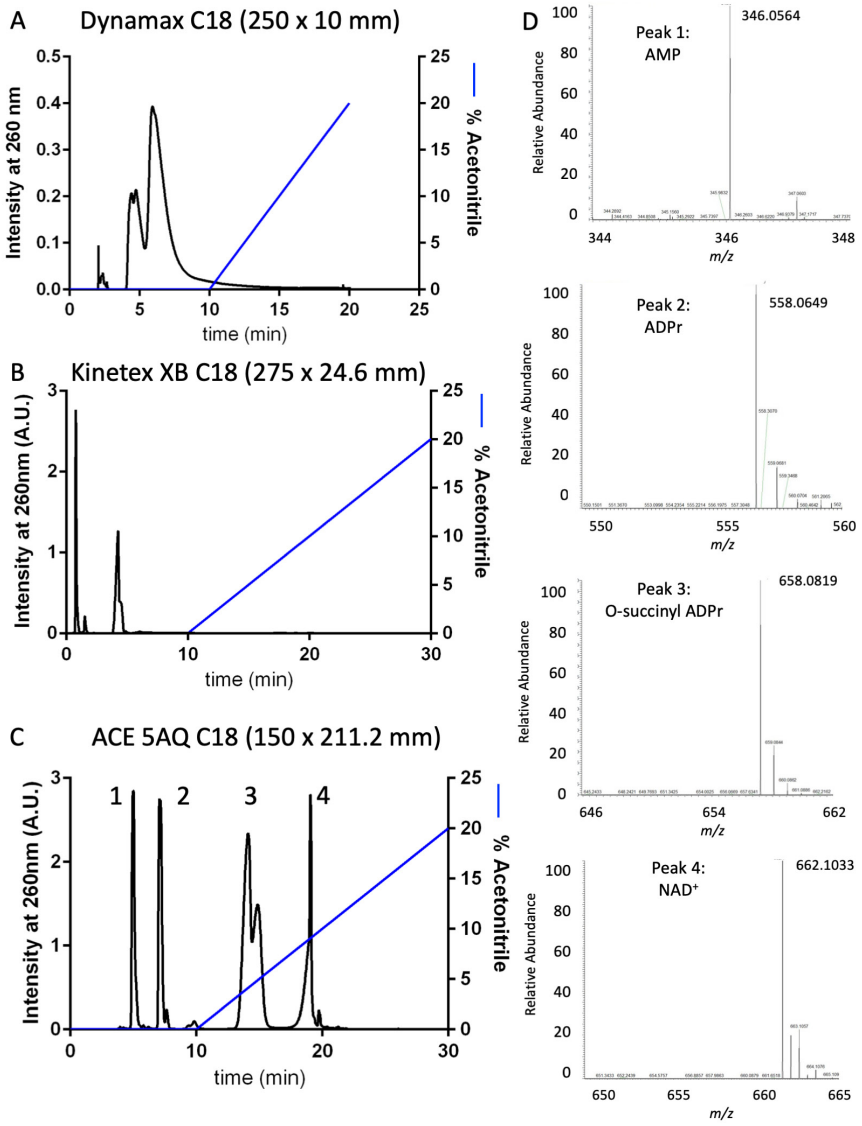

Figure 2.6 HPLC purification of O-succinyl ADPr. 200 µM succinylated histone H2B, 50 µM SIRT5 in reaction buffer, pH 8, and 2 mM NAD^+ incubated at 37°C for 1 hour and quenched with 150 µM TFA. Supernatant was loaded onto HPLC columns: A) Dynamax C18 column, B) Kinetex C18, and C) ACE 5AQ and eluted with acetonitrile gradient. Fractions 1-4 from the ACE 5AQ C18 column were collected and analyzed by mass spectrometry. Fractions were identified as the following in Panel D: 1) AMP 2) ADPr 3) O-succinyl ADPr and 4) NAD^+.

Purity of O-succinyl ADPr by ^{1}H-NMR

To assess the purity of O-succinyl ADPr following HPLC separation, unlabeled and ^{13}C-labled O-succinyl ADPr were evaluated by ^{1}H- NMR (Fig. 2.7). Chemical shifts from the succinyl group are upfield at 2.8 ppm, shifts from the ribose and the phosphate hydroxyls are grouped together in the 4 to 6 ppm range, and the aromatic adenine hydrogens are clearly detected around 8.5 ppm. The sample does not additional signal for the nicotinamide protons expected from NAD^{+}, which would appear in the 8-10ppm range, confirming that separation from NAD^{+} was achieved during HPLC purification.

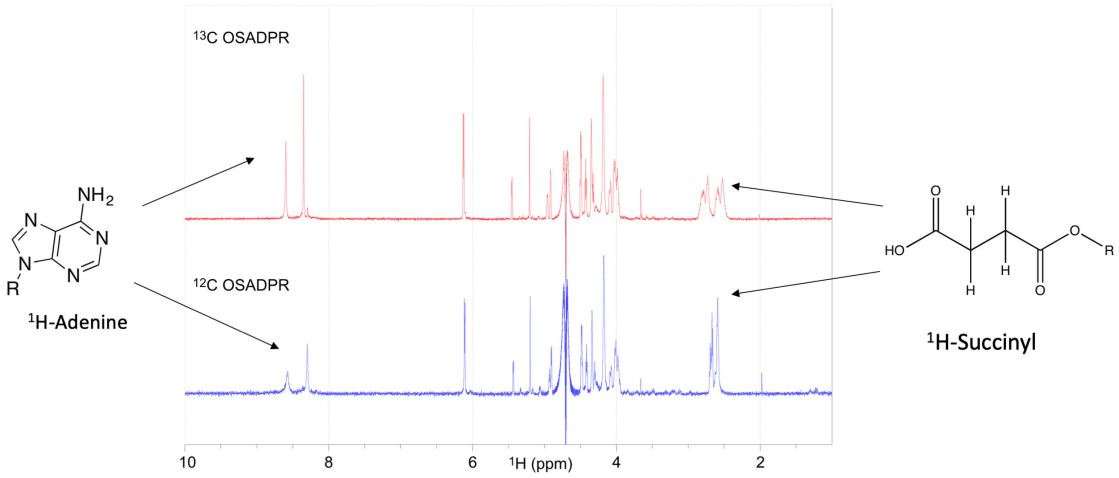

Figure 2.7: ^{1}H Spectra of ^{13}C (top) and ^{12}C O-succinyl ADPr (bottom). In both spectra, succinyl protons are upfield at 2.8 ppm, and aromatic protons from adenine are downfield at 8.5 ppm. Purity from NAD^+ is assessed in the aromatic region. Two peaks are expected from adenine; nicotinamide ring from NAD^+ would show additional peaks in this region.

2.4 References

Aitken, A. and M. Learmonth (1996). Succinylation of Proteins. The Protein Protocols Handbook. J. M. Walker. Totowa, NJ, Humana Press**:** 343-344.

Aravind, L., R. Mazumder, S. Vasudevan and E. V. Koonin (2002). "Trends in protein evolution inferred from sequence and structure analysis." Curr Opin Struct Biol **12**(3): 392-399.

Avalos, J. L., I. Celic, S. Muhammad, M. S. Cosgrove, J. D. Boeke and C. Wolberger (2002). "Structure of a Sir2 enzyme bound to an acetylated p53 peptide." Mol Cell **10**(3): 523-535.

Bheda, P., S. Swatkoski, K. L. Fiedler, J. D. Boeke, R. J. Cotter and C. Wolberger (2012). "Biotinylation of lysine method identifies acetylated histone H3 lysine 79 in Saccharomyces cerevisiae as a substrate for Sir2." Proc Natl Acad Sci U S A **109**(16): E916-925.

de Souza, R. F. and L. Aravind (2012). "Identification of novel components of NAD-utilizing metabolic pathways and prediction of their biochemical functions." Mol Biosyst **8**(6): 1661-1677.

Du, J., Y. Zhou, X. Su, J. J. Yu, S. Khan, H. Jiang, J. Kim, J. Woo, J. H. Kim, B. H. Choi, B. He, W. Chen, S. Zhang, R. A. Cerione, J. Auwerx, Q. Hao and H. Lin (2011). "Sirt5 is a NAD-dependent protein lysine demalonylase and desuccinylase." Science **334**(6057): 806-809.

Frye, R. A. (2000). "Phylogenetic classification of prokaryotic and eukaryotic Sir2-like proteins." Biochem Biophys Res Commun **273**(2): 793-798.

Hallows, W. C., S. Lee and J. M. Denu (2006). "Sirtuins deacetylate and activate mammalian acetyl-CoA synthetases." Proc Natl Acad Sci U S A **103**(27): 10230-10235.

Hirschey, M. D., T. Shimazu, J. A. Capra, K. S. Pollard and E. Verdin (2011). "SIRT1 and SIRT3 deacetylate homologous substrates: AceCS1,2 and HMGCS1,2." Aging (Albany NY) **3**(6): 635-642.

Iyer, L. M., V. Anantharaman, M. Y. Wolf and L. Aravind (2008). "Comparative genomics of transcription factors and chromatin proteins in parasitic protists and other eukaryotes." Int J Parasitol **38**(1): 1-31.

Jackson, M. D. and J. M. Denu (2002). "Structural identification of 2'- and 3'-O-acetyl-ADP-ribose as novel metabolites derived from the Sir2 family of beta -NAD+-dependent histone/protein deacetylases." J Biol Chem **277**(21): 18535-18544.

Lee, S., L. Tong and J. M. Denu (2008). "Quantification of endogenous sirtuin metabolite O-acetyl-ADP-ribose." Anal Biochem **383**(2): 174-179.

Luger, K., T. J. Rechsteiner and T. J. Richmond (1999). "Expression and purification of recombinant histones and nucleosome reconstitution." Methods Mol Biol **119**: 1-16.

Park, J., Y. Chen, Daniel X. Tishkoff, C. Peng, M. Tan, L. Dai, Z. Xie, Y. Zhang, Bernadette M. M. Zwaans, Mary E. Skinner, David B. Lombard and Y. Zhao (2013). "SIRT5-Mediated Lysine Desuccinylation Impacts Diverse Metabolic Pathways." Molecular Cell **50**(6): 919-930.

Ringel, A. E., C. Roman and C. Wolberger (2014). "Alternate deacylating specificities of the archaeal sirtuins Sir2Af1 and Sir2Af2." Protein Sci **23**(12): 1686-1697.

Sauve, A. A., I. Celic, J. Avalos, H. Deng, J. D. Boeke and V. L. Schramm (2001). "Chemistry of gene silencing: the mechanism of NAD+-dependent deacetylation reactions." Biochemistry **40**(51): 15456-15463.

Szczepankiewicz, B. G., K. J. Koppetsch and R. B. Perni (2011). "One-step, nonenzymatic synthesis of O-acetyl-ADP-ribose and analogues from NAD and carboxylates." J Org Chem **76**(16): 6465-6474.

Zhang, Z., M. Tan, Z. Xie, L. Dai, Y. Chen and Y. Zhao (2011). "Identification of lysine succinylation as a new post-translational modification." Nat Chem Biol **7**(1): 58-63.

Chapter 3
O-succinyl ADPr Stability and Metabolomics Studies

3.1 Introduction

A PubMed search on "O-succinyl ADP ribose" returns zero publications. Although many researchers have studied sirtuins that catalyze the NAD^+-dependent removal of succinyl groups from lysines, little is known about the metabolic fate of the NAD^+-derived product, O-succinyl ADPr. However, several enzymes have been shown to metabolize O-acetyl ADPr (summarized in Chapter 1) by removing the acetyl chain or by cleaving the adenosine diphosphate bond. More recently, Peterson and colleagues found that the macrodomain protein, C6orf130, catalyzes the removal of the acyl group from O-acetyl-ADPr, O- propionyl-ADPr, and O-buturyl ADPr (Peterson, Chen et al. 2011). Macrodomain proteins, like sirtuins, are also ancient proteins found in all three domains of life, some of which catalyze the removal of ADPr moieties (Rack, Perina et al. 2016). In lower organisms such as a bacteria, macrodomain proteins are often found in the same operon as sirtuins (Chen, Vollmar et al. 2011) suggesting they may function in the same metabolic pathway. However, in these studies, a clear biological role for O-acyl ADPr metabolite has yet to be determined.

I hypothesized that the biological role of O-acyl ADPr is to act as a carrier molecule, shuttling acyl chains into downstream metabolic pathways. My goals were to 1) determine the natural breakdown rate of newly synthesized O-succinyl ADPr, 2) look for evidence that *E. coli* cell lysates metabolize O-succinyl ADPr, and 3) search for metabolites that have incorporated the isotopic label for the acyl chain on O-succinyl ADPr. Using the mass spectrometry detection method developed in Chapter 2, I was able to determine the relative stability of the newly synthesized O-succinyl ADPr. In collaboration with Drs. Tao Huan and Gary Suizdak (Scripps

Research Institute), we found evidence that O-succinyl ADPr is metabolized by *E. coli* cell lysates at a faster rate than the natural breakdown of the molecules. In a preliminary metabolomics study, we found that the primary metabolite product of O-succinyl ADPr observed in *E. coli* lysates is succinate.

3.2 Methods

Stability of O-succinyl ADPr in water

O-succinyl ADPr was lyophilized straight from HPLC and bought up in MilliQ water to approximately 200 μM. All concentrations are estimates based on amount of NAD^+ reacted as calculated from the G6PD enzyme-coupled assay described (Avalos, Celic et al. 2002). Samples were quenched with 4x methanol:acetonitrile:water (2:2:1) and immediately flash frozen in liquid nitrogen. Samples were lyophilized, and analyzed by LC-MS or LC-MS/MS.

Time Course Studies

Time course reactions contained approximately 50 μM O-succinyl ADPr in either 50 mM Tris HCl, pH 7.4 plus 5mM DTT, Phosphate Buffered Saline (PBS) plus 5mM DTT, pH 7.4 or *E. coli* cell lysates plus 5mM DTT. PBS contains from 137 mM NaCl, 2.7 mM KCl, 10.1 mM $NaHPO_4$, and 1.76 mM NaH_2PO_4. *E. coli* K12 MG1655 were grown in 50 mL Luria Bertani (LB) medium at 37°C to OD_{600} of 1.0. Cells were spun at 4000*g* for 10 minutes at 4°C, rinsed with PBS and reconstituted in PBS containing 5mM DTT. Cells were lysed by sonication in an ice water bath containing calcium chloride to ensure the temperature did not rise above 25°C during sonication. The sonication method was first was validated by OD_{600} in test cell lysates to ensure a minimum of 95% lysis. After sonication, lysates were immediately transferred to cold

O-succinyl ADPr and placed in a 37°C water bath. All time points were processed by quenching with 4x methanol:acetonitrile:water (2:2:1) and immediately flash frozen in liquid nitrogen. Samples were lyophilized and analyzed by LC-MS.

Liquid Chromatography – Mass Spectrometry (LC-MS)

O-succinyl ADPr depletion was monitored by LC-MS. Reconstituted samples were resolved with a PolyHydroxyethyl A, HILIC column (300 Å, 200 x 2.1mm, PolyLC Inc, Nest group) using a Dionex UltiMate 3000 µHPLC system coupled to a Q-Exactive benchtop Orbitrap mass spectrometer (Thermo Scientific) in negative ion mode. A gradient of 10 mM ammonium acetate, pH 4.5 (mobile A) and acetonitrile (mobile B) was used. All samples analyzed on the Q-Exactive were obtained in full-MS acquisition mode. The mass spectrometer parameters were optimized using a direct infusion of ≈ 0.01 M O-succinyl ADPr in 50% acetonitrile with a flow of 0.4 ml/min. The electrospray ionization source parameters were set as follows: sheath gas flow rate 9, Spray voltage 3.2 kV, capillary temperature 320 °C, probe temperature 300 °C, auxiliary gas 0, auxiliary gas heater temperature 30 °C, collision energy 0 eV. Analysis was performed on Xcalibur Qual browser software.

Liquid Chromatography tandem mass spectrometry (LC-MS/MS)

O-succinyl ADPr depletion was also monitored by LC-MS/MS (Fig 3.2 only). Reconstituted samples were resolved with a PolyHydroxyethyl A, HILIC column (300 Å, 200 x 2.1mm, PolyLC Inc, Nest group) using a TSQ Vantage Triple Stage Quadrupole mass spectrometer (Thermo Scientific) in negative ion mode. A gradient of 10 mM ammonium acetate, pH 4.5 (mobile A) and acetonitrile (mobile B) was used. All samples detected on the

TSQ Vantage were obtained using selected reaction monitoring. The transition used was *m/z* 658>346 with a collision energy of 30 eV and a Q1 peak width of ± 0.7 *m/z.* The mass spectrometer parameters were optimized using a direct infusion of ≈ 0.01 M O-succinyl ADPr in 50% acetonitrile with a flow rate of 0.4 ml/min. The electrospray ionization source parameters were set as follows: sheath gas pressure 40, Vaporizer temperature 381 °C, Spray voltage 2.5 kV, ion sweep gas pressure 2.0, capillary temperature 206 °C, auxiliary gas pressure 25. Analysis was performed on Xcalibur Qual browser software.

Metabolomics

Samples sent to the Scripps Research Institute were prepared as described in 'Time Course Studies', but shipped on dry ice following quenching in 4x methanol:acetonitrile:water (2:2:1), and flash freezing in liquid nitrogen. Samples were analyzed by RPLC (reverse-phase liquid chromatography) and HILIC ESI-QTOFMS (hydrophilic interaction liquid chromatography electrospray ionization quadrupole time-of-flight mass spectrometry) as previously described (Ivanisevic, Zhu et al. 2013). O-succinyl ADPr metabolic products were extracted by comparing the study results of unlabeled O-succinyl ADPr in cell lysates to ^{13}C-labeled O-succinyl ADPr in cell lysates.

3.3 Results

Stability of O-succinyl ADPr

After synthesizing and purifying both unlabeled and ^{13}C-labeled O-succinyl ADPr (outlined in Chapter 1), I wanted to understand the natural breakdown rate of it following HPLC purification. To do so, I reconstituted two identical samples in water, which had been previously

lyophilized immediately following HPLC purification. As shown in figure 3.1 A-D, one sample sat at room temperature and time points were taken every 24 hours. Another identical sample, figure 3.1 E-F, underwent one freeze/thaw cycle where the sample was flash frozen in liquid nitrogen and allowed to thaw at room temperature. The peak area of O-succinyl ADPr was analyzed over time using the LC-MS method developed in chapter 2. As shown in figure 3.1 A-D, there was gradual appearance of a second peak in the sample that sat at room temperature. This was reassuring since others had confirmed that O-acetyl ADPr undergoes a sirtuin independent transesterification, equilibrating the 2' and 3' O-acetyl ADPr species (Sauve, Celic et al. 2001, Jackson and Denu 2002). However, due to the appearance of the second peak, quantitating peak area change over time was challenging, and interpretation of this set of time course data was limited. The peak area increased (Panels A-C) before decreasing (Panel D). However, I concluded that O-succinyl ADPr was not immediately falling apart, and I could proceed with physiologically relevant experiments. The peak area of the sample that underwent one freeze/thaw cycle, figure 3.1 E-F decreased 10-fold after just one freeze/thaw cycle, which led me to limit any future liquid freeze/thaw cycles in the future.

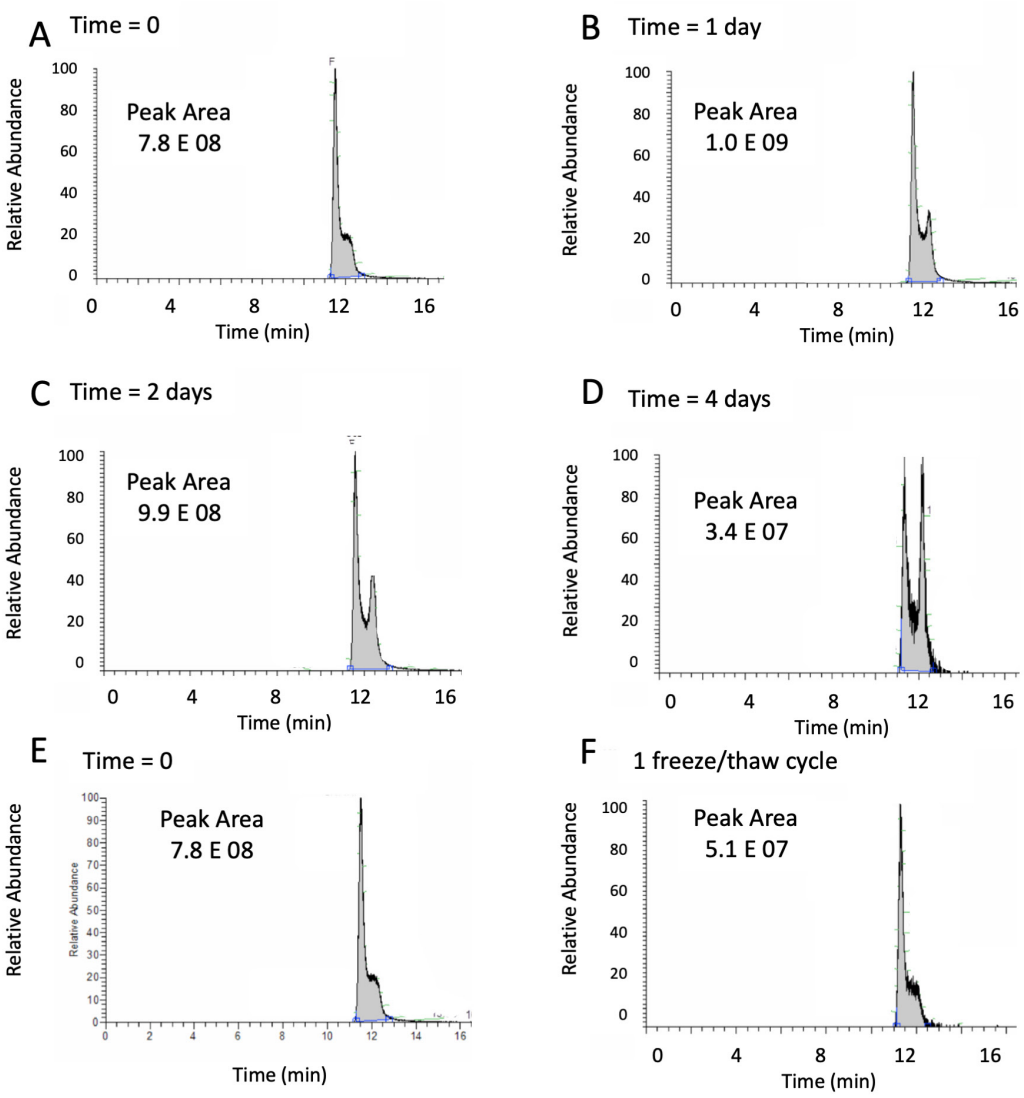

Figure 3.1 Timecourse analysis of O-succinyl ADPr in water. Extracted ion chromatograms of O-succinyl ADPr, m/z = 658.0108 +/- 2ppm. Roughly 200 µM O-succinyl ADPr reconstituted in water, pH 4.5 (due to residual TFA from HPLC purification) sitting on benchtop for 4 days (A-D) and through 1 freeze/thaw cycle (E-F). Data acquired on a Q-Exactive benchtop Orbitrap mass spectrometer (Thermo Scientific). Peak area was drawn manually.

Timecourse Analysis of O-succinyl ADPr in Phosphate Buffered Saline

It was important to the determine decomposition rate of O-succinyl ADPr in PBS as a baseline before tracking decomposition of O-succinyl ADPr in *E. coli* cell lysates in PBS. O-succinyl ADPr was incubated in PBS, pH, 7.4, at 37 °C, and time points were taken at 0, 0.5,1, 2, 4, and 7 hours (Fig. 3.2) in triplicate. Peak area was analyzed by LC-MS/MS, and representative peak areas at time equal to 0 and 7 hours are shown in figure 3.2, panels A and B respectively. As shown in figure 3.2C, over 7 hours at 37 °C in PBS, O-succinyl ADPr decreases 5-fold. Even though the general trend of O-succinyl ADPr decreased over time, the data was not linear and contained large standard deviations from the mean. To remedy this, it was suggested to spike in a stable metabolite, glucose, as an internal standard, which is easy to detect by mass spectrometry. In the second time course experiment, O-succinyl ADPr was incubated in PBS, pH 7.4, at 37°C with the addition of 100 µM glucose, and time points were taken at 0, 0.5,1, 2, and 4 hours in triplicate. Data was collected by LC-MS in full-MS acquisition mode to search for possible degradation products of O-succinyl ADPr. Example *m/z* and chromatograms are shown of O-succinyl ADPr at time equal to 0 and 4 hours in Figure 3.3A. The primary degradation product found was ADPr, with a *m/z* = 558.0644 ± 2ppm shown in figure 3.3B. The chromatogram of ADPr at time equal to 0 is undetectable, but increases to a peak area of 1E07 after 4 hours. A possible explanation for what was going on in solution is hydrolysis of the ester linkage of the succinyl group on ADPr. As shown in figure 3.3C, the internal standard, glucose, allowed for normalization of peak are and O-succinyl showed a linear decrease over time with a 30% loss in peak area in the 4-hour incubation period. This result provided a foundation on how O-succinyl ADPr decomposes naturally in PBS without the addition of cellular extracts.

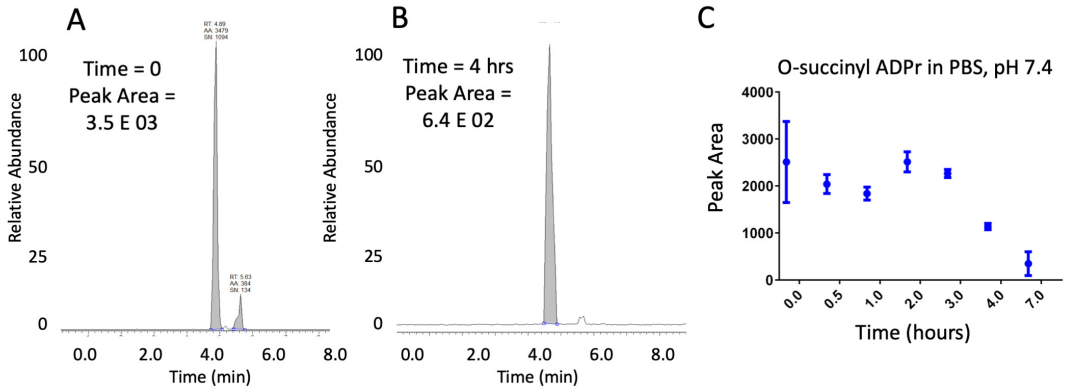

Fig. 3.2 Timecourse of O-succinyl ADPr in PBS, pH 7.4. Example chromatograms of time = 0 and time = 7 hours, and graphical representation of mean ± SD peak area of one experiment performed in triplicate. Roughly 50 µM of O-succinyl ADPr was reconstituted in PBS, pH 7.4 incubated at 37°C. Data aquired on a TSQ Vantage Triple Stage Quadrupole mass spectrometer (Thermo Scientific) (*m/z* 658>346*)*.

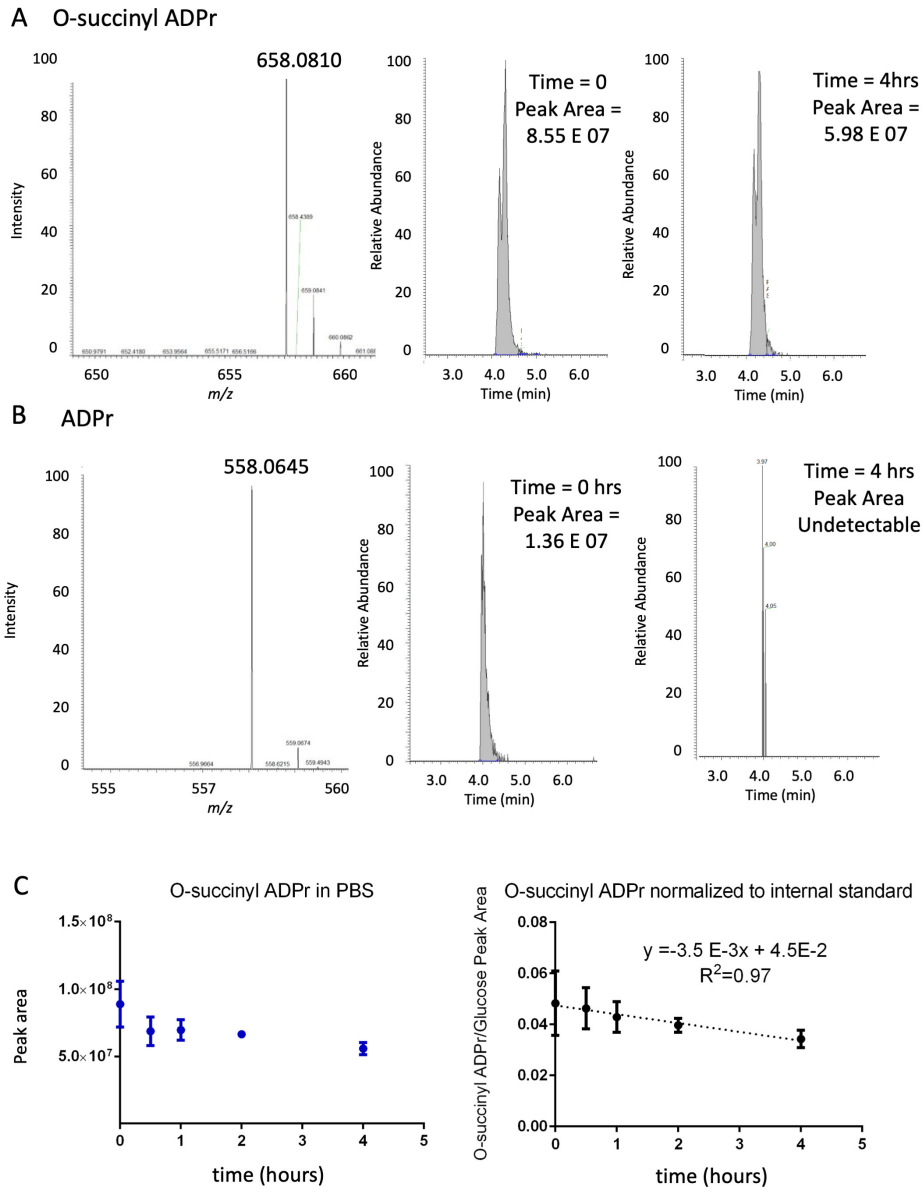

Figure 3.3 Second timecourse of O-succinyl ADPr in PBS, pH 7.4. Example *m/z* spectra and chromatograms of O-succinyl ADPr (A) and ADPr (B) at time = 0 and time = 4 hours. Graphical representation of mean ± SD of peak area over time (C left) and peak area normalized by internal standard, glucose, peak area (C right). Data acquired on a Q-Exactive benchtop Orbitrap mass spectrometer (Thermo Scientific), m/z = 658.0804 ± 2ppm (O-succinyl ADPr), 558.0650 ± 2ppm (ADPr).

Timecourse Analysis of O-succinyl ADPr in E.coli cell lysates

After determining that 30% of O-succinyl ADPr would break down in PBS alone, we wished to see if this rate would change in *E. coli* cell lysates or in a different buffer. In collaboration with Drs. Gary Siuzdak and Tao Huan, we monitored the disappearance of O-succinyl ADPr in PBS, Tris HCL, pH 7.4 and *E. coli* cell lysates. Samples were sent to Scripps Center for Metabolomics for analysis by mass spectrometry. Peaks obtained by the column used by Dr. Tao Huan (Aquity UPLC BEH, Waters) were sharp and lacked the second peak I had seen using the HILIC column (Fig3.4D). Figure 3.4A shows that O-succinyl ADPr in PBS fluctuated over a range of 6E05 to 9E05. This was consistent with the fluctuations I had seen previously without an internal standard, but we were surprised that the overall trend did not show a decrease in O-succinyl ADPr as I had seen in my previous time course experiments. Interestingly, as shown in figure 3.4B, O-succinyl ADPr in Tris-HCl buffer was depleted about 3-fold. This was a surprising result, and we decided to not pursue more experiments with Tris-HCl. Significantly, O-succinyl ADPr in cell lysates showed a very clear exponential decrease to about 50% relative abundance over 4 hours (Fig 2.4 C). One explanation for this trend is *E. coli* cell lysates were metabolizing O-succinyl ADPr. This merited follow-up experiments to try to identify possibly metabolic products of O-succinyl ADPr.

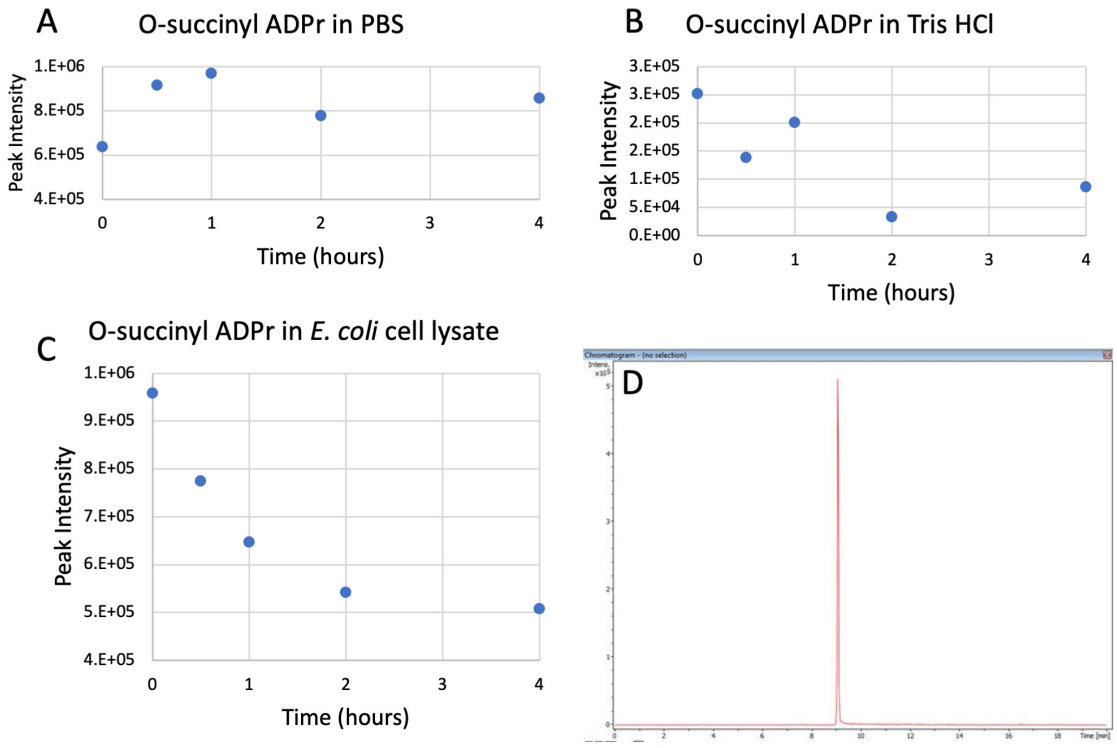

Figure 3.4 Consumption of O-succinyl ADPr in PBS, Tris-HCl and *E.* coli cell lysates. All data points represent LC peak height as shown in panel D. pH of all samples was 7.4. Data provided by Tao Huan, Scripps Metabolomics Institute.

Metabolomics analysis of O-succinyl ADPr in E.coli cell lysates

Since there was evidence that *E. coli* cell lysates were metabolizing O-succinyl ADPr, we did a preliminary search for metabolites. We tested the following five conditions: *E. coli* cell lysates alone, lysates with ^{13}C-labeled O-succinyl ADPr, lysates with unlabeled O-succinyl ADPr, lysates with ^{13}C-labeled succinic acid, PBS with unlabeled O-succinyl ADPr. All samples were prepared in replicates of five and sent to Scripps Center for Metabolomics for analysis by Dr. Tao Huan. Dr. Huan analyzed the samples as outlined in (Ivanisevic, Zhu et al. 2013). Consistent with the initial time course results, the peak intensity of O-succinyl ADPr in PBS decreased about by about one-third in 4 hours (Fig. 3.5 C), and the thermally more stable product, ADPr formed (Fig 3.5 D). However, inconsistent with previous results, O-succinyl ADPr peak intensity in lysates also decreased by about one-third over 4 hours (Fig. 3.5 A and C), but the formation of ADPr in cell lysates did not significantly increase or decrease. This could mean that the enzymatic reactions of ADPr could be contributing to the metabolism of O-succinyl ADPr in lysates. One way to check this would be to compare this result to the natural abundance of ADPr in cell lysates alone.

In order to search for metabolic products, Dr. Huan compared the metabolic products from the unlabeled and ^{13}C-labeled O-succinyl ADPr in lysates experiments. He searched for metabolites containing the four possible mass differences (1.0034, 2.0067, 3.0100, 4.0134 *m/z*). However, there was one major issue with the setup of the experiment; 0.2 mgs of O-succinyl ADPr was weighed to dose *E. coli* cell lysates and PBS on an analytical balance. This resulted in the initial dosing amount of ^{13}C O-succinyl ADPr to be about half of the initial dosing amount of ^{12}C O-succinyl ADPr (Fig. 3.6). Since the dynamic range of the ^{13}C sample was much narrower than that of the ^{12}C sample, it is possible that metabolites were missed in this analysis. The

primary metabolic product of O-succinyl ADPr detected in this experiment was succinate. This is logical since preliminary studies showed O-succinyl ADPr degrading to ADPr in buffer. In a future experiment, we could measure relative amounts of O-succinyl ADPr via mass spectrometry for dosing instead of weighing.

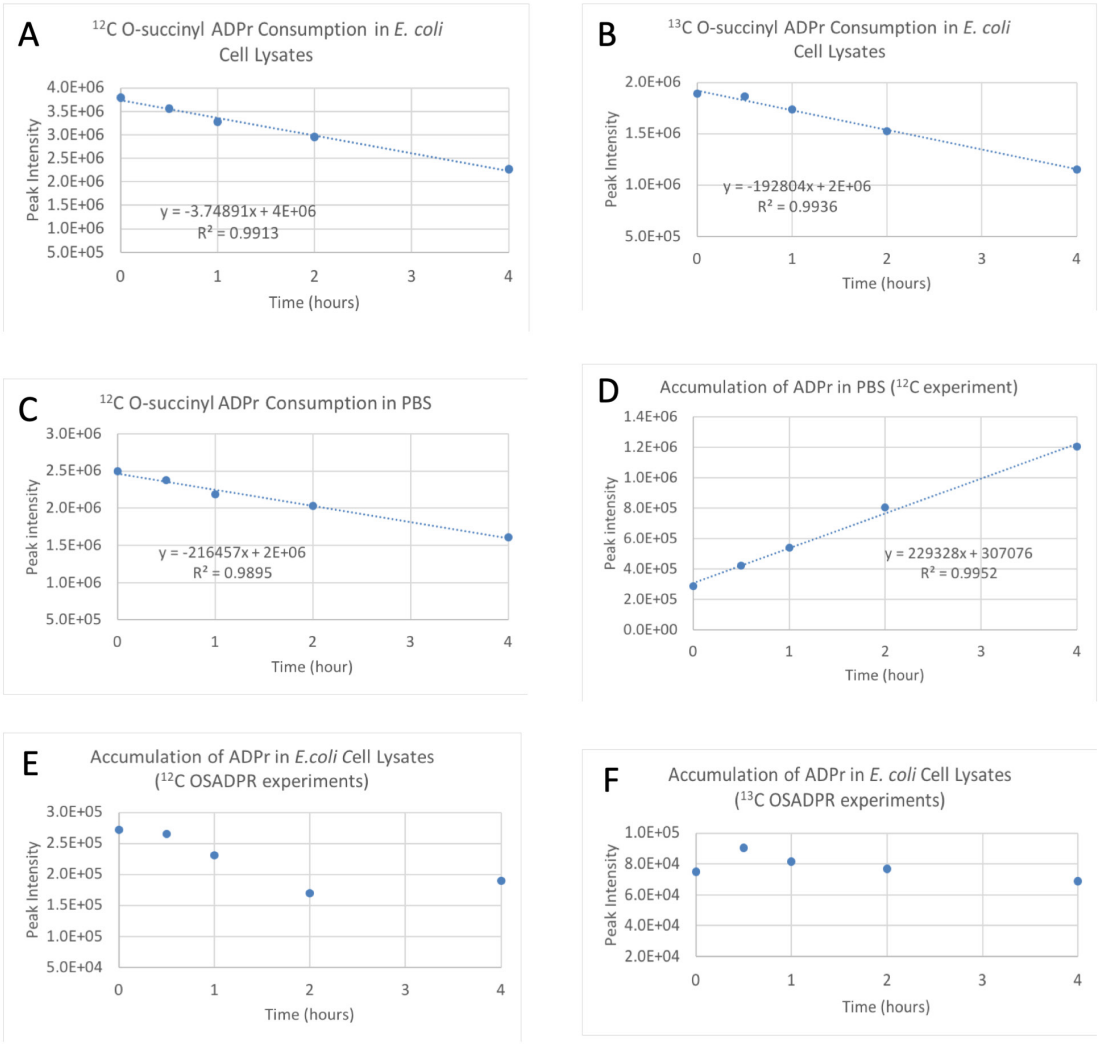

Figure 3.5 Consumption of O-succinyl ADPr and accumulation of ADPr in *E. coli* cell lysates and PBS measured by LC-MS. All data points represent the average of 5 replicates LC peak height. pH of all samples was 7.4. Data provided by Tao Huan, Scripps Metabolomics Institute.

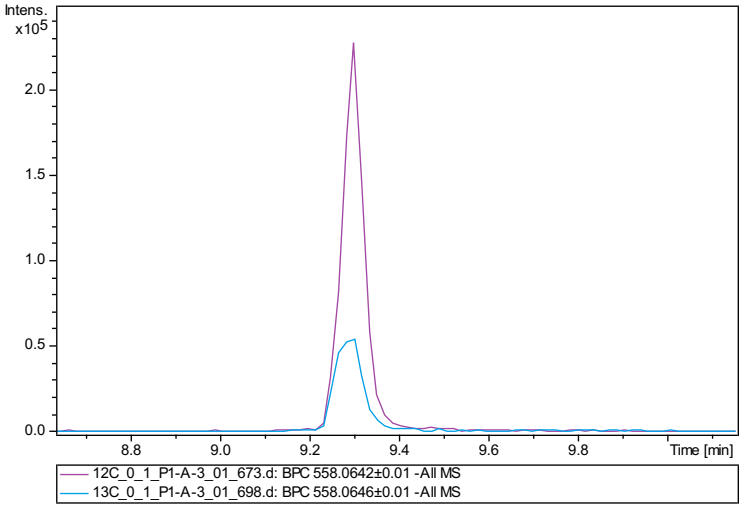

Figure 3.6 Chromatogram of initial dosing of ^{13}C-labeled (light blue) and unlabeled (magenta) O-succinyl ADPr. Initial dosing of amount of ^{13}C O-succinyl ADPr is roughly half that of unlabeled. This became an issue for the comparison of ^{12}C peak and ^{13}C peak as the ratio of these two intensities are not 1:1. Data courtesy of Tao Huan, Scripps Center for Metabolomics

3.4 References

Avalos, J. L., I. Celic, S. Muhammad, M. S. Cosgrove, J. D. Boeke and C. Wolberger (2002). "Structure of a Sir2 enzyme bound to an acetylated p53 peptide." Mol Cell **10**(3): 523-535.

Chen, D., M. Vollmar, M. N. Rossi, C. Phillips, R. Kraehenbuehl, D. Slade, P. V. Mehrotra, F. von Delft, S. K. Crosthwaite, O. Gileadi, J. M. Denu and I. Ahel (2011). "Identification of macrodomain proteins as novel O-acetyl-ADP-ribose deacetylases." J Biol Chem **286**(15): 13261-13271.

Ivanisevic, J., Z. J. Zhu, L. Plate, R. Tautenhahn, S. Chen, P. J. O'Brien, C. H. Johnson, M. A. Marletta, G. J. Patti and G. Siuzdak (2013). "Toward 'omic scale metabolite profiling: a dual separation-mass spectrometry approach for coverage of lipid and central carbon metabolism." Anal Chem **85**(14): 6876-6884.

Jackson, M. D. and J. M. Denu (2002). "Structural identification of 2'- and 3'-O-acetyl-ADP-ribose as novel metabolites derived from the Sir2 family of beta -NAD+-dependent histone/protein deacetylases." J Biol Chem **277**(21): 18535-18544.

Peterson, F. C., D. Chen, B. L. Lytle, M. N. Rossi, I. Ahel, J. M. Denu and B. F. Volkman (2011). "Orphan macrodomain protein (human C6orf130) is an O-acyl-ADP-ribose deacylase: solution structure and catalytic properties." J Biol Chem **286**(41): 35955-35965.

Rack, J. G., D. Perina and I. Ahel (2016). "Macrodomains: Structure, Function, Evolution, and Catalytic Activities." Annu Rev Biochem **85**: 431-454.

Sauve, A. A., I. Celic, J. Avalos, H. Deng, J. D. Boeke and V. L. Schramm (2001). "Chemistry of gene silencing: the mechanism of NAD+-dependent deacetylation reactions." Biochemistry **40**(51): 15456-15463.

Chapter 4

Conclusion and Future Directions

4.1 Conclusion and Future Directions

The longstanding mystery of why sirtuins, the ancient family of deacylase enzymes, requires the cofactor NAD^+, is a fascinating area of research which we are just beginning to understand. As shown in numerous studies, sirtuins play important roles in many aspects of biology (Sebastian, Satterstrom et al. 2012). Discovering the true role of NAD^+ will help us elucidate the overall function of all sirtuins and will establish links between sirtuin activity and cellular metabolism. Since the discovery that sirtuins remove a variety of acyl chains, the understanding of their biological roles has expanded beyond that of a simple histone deacetylase enzyme.

I have taken the first step to uncover potential metabolic pathways that utilize the acyl groups carried by O-acyl ADPr. I have developed a method to synthesize, purify, and detect O-succinyl ADPr with an isotopic label on the acyl group. Because of this method takes advantage of the intrinsic reactivity of acyl anhydrides, O-acyl ADPr can be synthesized with various acyl chains and isotopic label combinations. With the help of collaborators, we found initial evidence that O-succinyl ADPr is metabolized by *E. coli* cell lysates at a faster rate than the natural breakdown of the molecules in PBS. Additionally, we observed that the natural breakdown of O-succinyl ADPr to ADPr and succinate increased over time in PBS. However, in the cell lysate experiment, the level of ADPr remained constant. This could mean ADPr was being metabolized futher by the cell lysates. An experiment to test this would be to track the overall rate of ADPr in cell lysates compared to lysates dosed with O-succinyl ADPr.

Due to experimental errors in the metabolomics experiment the dynamic range was limited, and we did not find evidence that proves ADPr is a novel carrier shunting ADPr into a novel metabolic pathway. The analysis done by Dr. Haun showed the dominant metabolite of O-succinyl ADPr was succinate. Repeating the experiment with relative amounts of O-succinyl ADPr via measured mass spectrometry instead of weighing would solve this problem. Additionally, an important future experiment will be determining the effect of free succinate versus O-succinyl ADPr on cell metabolism. This experiment would differentiate O-succinyl ADPr's role in the cell from succinates. Lastly, O-succinyl ADPr was chosen as a model metabolite because succinylation is found widely spread across organisms in all three domains of life (Zhang, Tan et al. 2011, Park, Chen et al. 2013). There are many acylation sites in a wide variety of organisms (Ch. 2), and using a different acyl chain such as a long fatty acyl chain or a different model organism may turn up a different pathway. These experiments would provide a more well-rounded investigation into the metabolic fate of the acyl chain.

4.2 References

Park, J., Y. Chen, Daniel X. Tishkoff, C. Peng, M. Tan, L. Dai, Z. Xie, Y. Zhang, Bernadette M. M. Zwaans, Mary E. Skinner, David B. Lombard and Y. Zhao (2013). "SIRT5-Mediated Lysine Desuccinylation Impacts Diverse Metabolic Pathways." Molecular Cell **50**(6): 919-930.

Sebastian, C., F. K. Satterstrom, M. C. Haigis and R. Mostoslavsky (2012). "From sirtuin biology to human diseases: an update." J Biol Chem **287**(51): 42444-42452.

Zhang, Z., M. Tan, Z. Xie, L. Dai, Y. Chen and Y. Zhao (2011). "Identification of lysine succinylation as a new post-translational modification." Nat Chem Biol **7**(1): 58-63.

Curriculum Vitae

Elyse Blazosky

Birth

February 11, 1989	Alamogordo, NM

Education

2015 - 2018	M.S. expected, Johns Hopkins University School of Medicine, Baltimore, MD. Program in Molecular Biophysics.
2007 – 2013	B.S., Chemistry. B.M. Instrumental performance. Minor in Biology. University of Northern Colorado, Greeley, CO.

Research

2015 - 2018	Graduate Student, Johns Hopkins University School of Medicine, Baltimore, MD, under Prof. Cynthia Wolberger, Department of Biophysics and Biophysical Chemistry. Synthesis, purification and metabolic analysis of isotopically labeled, cellular metabolite.
2012 - 2013	Undergraduate Research Assistant, University of Northern Colorado, Greeley, CO under Prof. Mark Thomas. Performed basic protein biochemistry assays to evaluate ion channel protein expression levels in mouse models of Parkinson's disease.

Other Professional Experience

2013 - 2015	Clinical Lab Technologist, Mayo Clinic Endocrinology Laboratory, Rochester, MN. Extracted hormone analytes from patient serum specimens and quantitated using LC-MS/MS for diagnostic purposes.
2013	Developmental Chemist, Aspire Biotech Inc., Colorado Springs, CO. Developed and tested improved method of sterilization for medical grade cyanoacrylates.
2012	Summer Lab Assistant, Aspire Biotech, Colorado Springs, CO. Formulated and tested medical grade cyanoacrylates following GLP and GMP.

2007 – 2010	Clinical Lab Summer Student, Mayo Clinic Biochemical Genetics Laboratory, Rochester, MN. Prepared patient urine specimens for GC/MS analysis.
Peer-Reviewed Publications	Brickner, J. R., Soll, J. M., Lombardi, P. M., Va ̊gbø, C. B., Mudge, M. C., Oyeniran, C., Rabe, R., Jack- son, J., Sullender, M. E., **Blazosky, E.**, ... Mosammaparast, N. (2017). A ubiquitin-dependent signalling axis specific for ALKBH-mediated DNA dealkylation repair. Nature.
Presentations	Poster. What is the fate of O-acyl ADP ribose? Institute for Biophysical Research, Baltimore, MD 2017.
	Poster. Ion Channel Protein Expression in a Mouse Model of Parkinson's Disease. Undergraduate Science Symposium, Greeley, CO, 2013.
Certifications	Bronze Level Certification, Clinical Laboratory Quality Assurance Program Mayo Clinic, 2013.
Awards	
2013	Biological Sciences Research Grant, College of Natural and Health Sciences, University of Northern Colorado.
2012	Excellence in Analytical Chemistry, Department of Chemistry, University of Northern Colorado.
Outreach	
2016	Teaching Assistant, Hopkins Science Camp, Johns Hopkins School of Medicine, Baltimore, MD.
2014 - 2015	Volunteer Clinical Laboratory technologist, Mayo Clinic Free Clinic, Rochester, MN.
2014 - 2015	Musician, Music is Good Medicine, Mayo Clinic, Rochester, MN.